MIGMATITES OF THE EASTERN ADIRONDACK MOUNTAINS: NEW CONSTRAINTS ON THE TIMING, PETROLOGY, AND TECTONIC SETTING OF PARTIAL MELTING

MICHAEL L. WILLIAMS
Department of Geosciences, University of Massachusetts, Amherst, MA 01003

TIMOTHY W. GROVER
Department of Earth and Atmospheric Sciences, University of Northern Colorado, Greeley, CO 80639

CLAIRE R. PLESS
Department of Geosciences, University of Massachusetts, Amherst, MA 01003

KAITLYN A. SUAREZ
Department of Geosciences, University of Massachusetts, Amherst, MA 01003

SEAN P. REGAN
Department of Geosciences, University of Alaska Fairbanks, Fairbanks, AK 99775

GRAHAM B. BAIRD
Department of Earth and Atmospheric Sciences, University of Northern Colorado, Greeley, CO 80639

INTRODUCTION

The Adirondack Mountains of New York are a classic example of a high-grade, polydeformational terrane that has been used as an analog for mid/deep crustal continental collisional and extensional tectonism (Mezger, 1992; Selleck et al., 2005; Rivers, 2008). Numerous studies have characterized the nature and grade of metamorphism and deformation (Bohlen et al., 1985; Spear and Markussen, 1997; Storm and Spear, 2005). Many rocks show evidence for significant degrees of partial melting, and it seems likely that, at least in some rocks, significant amounts of melt have been lost from the local system. Previous workers have interpreted the melting to have occurred during one (or several) orogenic or thermal/magmatic events, but in many regions, questions remain about the timing, melt producing reactions, tectonic setting, and even the number of partial melting events. In order to interpret the tectonic history of the region and use the region as an analog for modern deep crust, it is critical to constrain the timing, setting, and rheologic implications of melting.

Migmatitic rocks in the eastern Adirondack Mountains can be very similar to one another in appearance. They tend to be gray-colored gneisses with layers of garnet-rich Qtz-Fsp-Sil-Bt gneiss interlayered with pink or white Qtz-Fsp leucosome with or without garnet. Leucosomes range from centimeters to a meter or more in width. The proportion of K-feldspar and plagioclase in both leucosome and gray gneiss varies widely. Many of the leucosomes are interpreted to be the product of in-situ melting although some have been interpreted to have been injected from outside of the local system (Bickford et al., 2008). Distinctive garnet- and sillimanite-rich gneisses with little biotite, “khondalite”, are relatively common, and are interpreted to be restitic rocks, where a significant amount of melt has been lost from the local rock.

The timing of melting is one of the critical outstanding questions in the Adirondack Mountains. Different rocks in different regions have been interpreted to have melted during one (or several) of four possible events: the 1190-1160 Shawinigan orogeny, the 1160-1140 AMCG intrusive event, the 1090-1050 Ottawan orogeny, or 1050-1030 extensional tectonism. In some regions, cross-cutting or contact relationships constrain the timing of melting although the interpretation is rarely unambiguous. In general, the gray gneisses and leucosomes form sub-parallel layers, and timing constraints tend to come from geochronology, particularly of zircon and monazite. Even though the migmatitic paragneisses can contain abundant zircon and monazite, interpretations of melting relationships are commonly constrained by relatively subtle textures and compositions of chronometer phases.

Multiscale compositional mapping combined with high-spatial-resolution (micron-scale), in-situ geochronology and geochemistry of monazite can provide significant insight into the nature of melting reaction(s), the timing of melting, the relationship to deformational events, and the ultimate significance of companion zircon geochronology (Williams et al., 2017). This field trip will visit localities in the eastern Adirondack Mountains where

we have applied this technique to samples of migmatite. The results suggest that melting did indeed occur at different times, producing rocks of very similar appearance. Although the relative intensity of the different events may have varied regionally, the degree of melting and melt segregation also played a role in controlling how fertile a rock was for melting in a subsequent event. The results presented here have a number of implications for the tectonic history of the region and for the rheology of the deep crust in general. They also provide a template for future studies in this region and in other regions in order to compare and interpret the tectonic setting of migmatitic rocks.

OVERVIEW OF ADIRONDACK GEOLOGY

The Grenville Province is a Proterozoic orogenic belt that represents the culminating continental collision(s) during assembly of the supercontinent of Rodinia (Rivers, 2008). The Grenville Province extends from northeastern Canada through the eastern and southern portion of the U.S. into Texas with proposed correlations in Australia, Antarctica, Baltica and others (Karlstrom et al., 1999). In eastern Canada, the Grenville Province forms a northeast trending belt approximately 2000 km long and 400-500 km wide. The Adirondack Mountains, located in northeastern New York, are a domical uplift of Mesoproterozoic rocks that are part of the Grenville Province (Fig. 1). The Green Mountain and Berkshire massifs represent outliers of the Grenville Province and lie to the east and southeast of the Adirondacks respectively.

The Adirondack Mountains have been divided into the Adirondack Lowlands and Highlands (Fig. 1), separated by the Carthage-Colton shear zone (Selleck et al., 2005). Most workers now recognize several major stages in the overall tectonic history (Fig. 2). The ca. (1300-1200 Ma) Elsevirian orogeny is interpreted to represent a period of arc and back-arc accretion on or near the margin of Laurentia (McLelland et al., 2013). The (ca.1180-1140 Ma) Shawinigan orogeny is interpreted to represent a period of accretionary orogenesis with closure of the Trans Adirondack Basin with subduction-related magmas forming above a westward-dipping subduction zone. The culminating collisional phase of the Shawinigan Orogeny is the result of the collision of the Adirondack Highlands-Green Mountain terrane with the Adirondack Lowlands terrane, which was part of the eastern margin of Laurentia. (Chiarenzelli et al., 2010). The effects of this orogenic event have been increasingly recognized in the Adirondack Lowland in recent years (Chiarenzelli et al., 2011) largely due to an expanding geochronologic database.

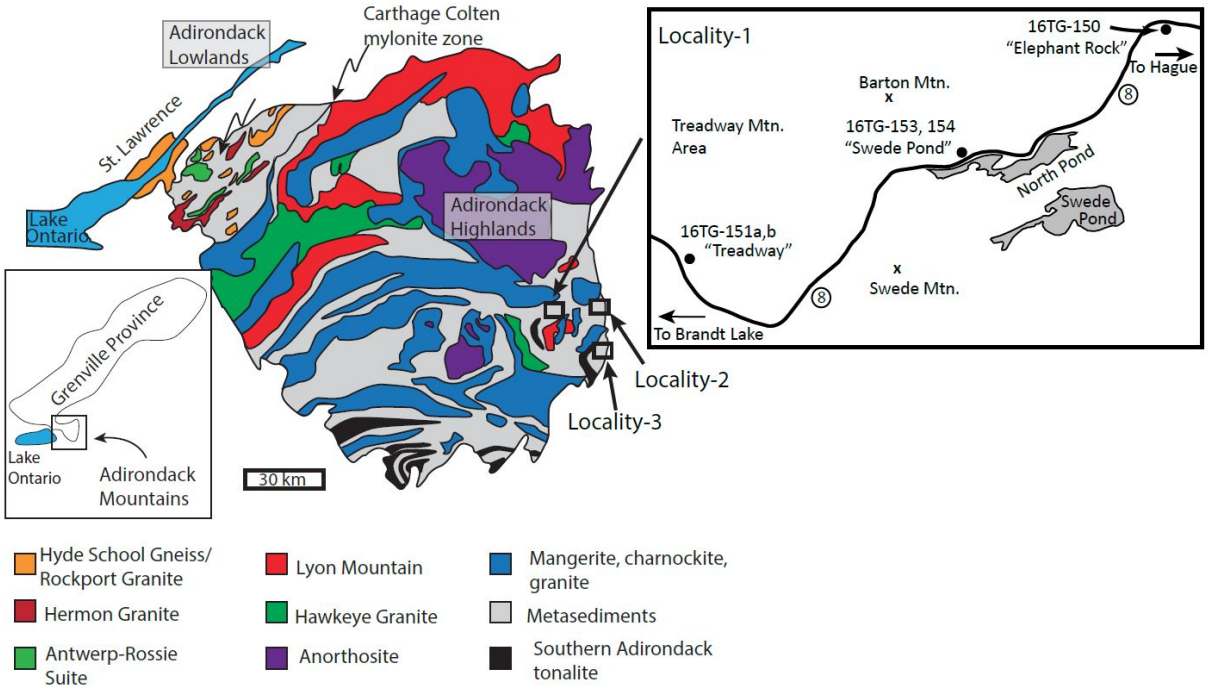

Figure 1. Generalized geologic map of the Adirondack Mountains (after McLelland, 2010) showing the location of the three main localities discussed in this paper. Inset shows the location of the three main outcrops discussed from Locality-1.

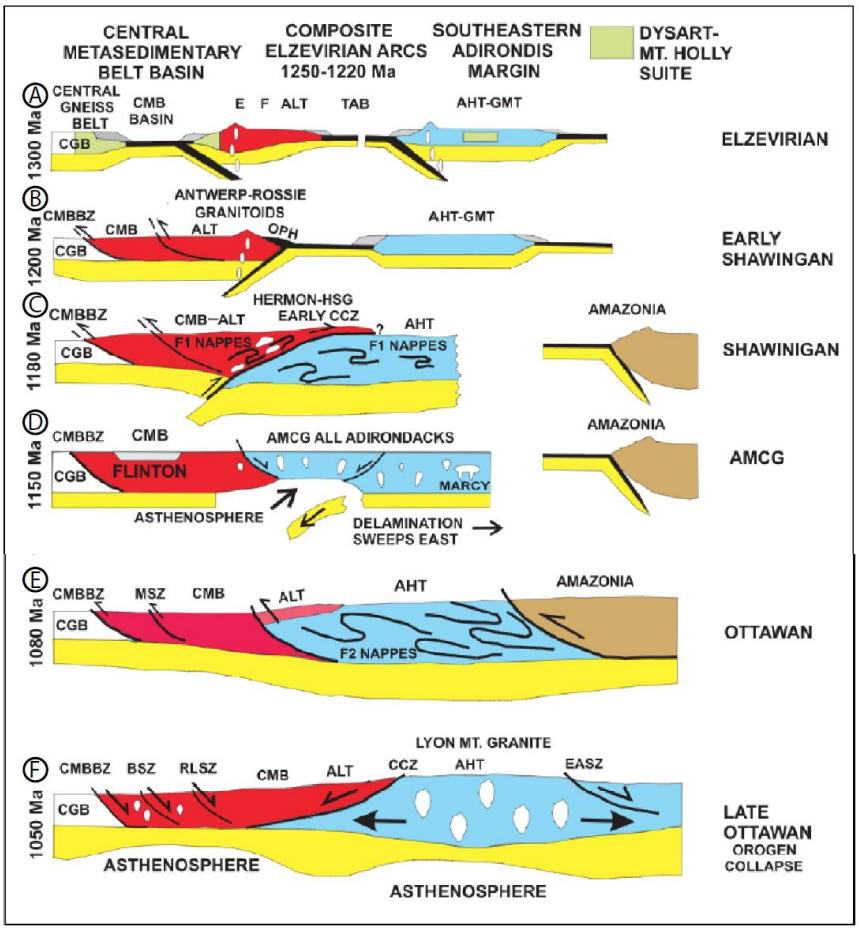

Figure 2. Schematic summary of the tectonic history of the Adirondack Mountains (Modified from McLelland, et al, 2013)

A voluminous suite of igneous rocks was emplaced near the end of the Shawinigan Orogeny (ca. 1155Ma). The magmatic event involved gabbro, anorthosite, mangerite, charnockite, and granite; the suite of intrusives is commonly referred to as the "AMCG suite". They are interpreted to be the result of lithospheric delamination (McLelland et al., 2004; Regan et al., 2011). The 3000 km^2 Marcy anorthosite massif (1154 +/- 6 Ma; McLelland et al. 2004; Hamilton et al. 2004), a member of this suite, is the dominant plutonic body in the Adirondack Highlands (Buddington, 1939).

The (ca. 1090-1030 Ma) Ottawan orogeny has been interpreted as a major continent-continent collision, involving large-scale thrusting and folding of rocks in the Adirondack Highlands (McLelland et al., 1996, 2001). Recently, however, at least the later part of the orogeny (<1050 Ma) has been interpreted as an extensional event with localized normal shearing on the Highlands-bounding, Carthage Colton and East Adirondack shear zones (Selleck et al., 2005; Wong et al., 2012; Regan et al., in review). The latest events in the cycle involved pegmatite emplacement, metasomatism, and local (ca, 980 Ma) disturbance. Tectonism during this final phase has been termed the Rigolet stage or orogeny (Rivers, 2008), which is currently interpreted to have had a minimal impact on the structural and metamorphic architecture in the Adirondack region.

In addition to plutonic rocks, the Adirondack Highlands contains abundant garnet-rich migmatitic gneisses, interpreted to have been derived from Al-rich sedimentary protoliths (Storm and Spear, 2005). Although leucosome layers, veins, and pods are common, many rocks are dominated by garnet (10s of percent), sillimanite, quartz, and feldspar, with variable amounts of prograde and retrograde biotite. Many of the biotite-poor, sillimanite-rich rocks have been termed "khondalite" (McLelland et al., 2002), and have been interpreted to be residues (restites), having lost some component of partial melt.

Bickford et al. (2008) and Heumann et al. (2006) carried out U-Pb zircon (IDTIMS) analyses, and Heumann combined in-situ monazite dating, in order to constrain the timing and setting of melting in the

Adirondack Highlands. Heumann et al. (2006) concluded that melting occurred primarily during the Shawinigan orogeny, which was cited as 1210-1160 Ma and also during AMCG magmatism, cited as 1165-1150 Ma. Bickford et al. (2008) investigated additional localities and concurred that melting occurred in many regions during the Shawinigan and AMGC events, but they also found evidence for melting at ca. 1050 Ma (Ottawan), particularly in the eastern Adirondack Highlands. They suggested that Ottawan metamorphic temperatures were probably high, but melting occurred only locally due to fluid influx or local decompression melting.

Samples discussed here and on the associated field excursion came from several commonly-visited localities in the eastern Adirondack Mountains. These include: Locality-1: outcrops along Route 8, west of Hague, NY, including the Elephant Rock, Swede Pond, and Treadway Mountain areas; Locality-2: the Dresden Station area along Rt. 22 south of Ticonderoga, NY; and Locality-3: outcrops along Route 22 south of Whitehall, NY. The Treadway Mountain area was also studied by Bickford et al., (2008), their Locality-9. Each of these localities contain migmatitic gray gneisses with abundant monazite and zircon. They represent a particularly appropriate target for in-situ monazite dating (i.e. "reaction dating", Williams et al., 2017), in order to evaluate the degree to which monazite analysis can provide insight into the melting history of these rocks.

METHODS

The outcrops described here have been visited on many field trips and described in numerous publications and field guides. For this study, oriented hand samples of gray garnet-rich gneisses with a variety of textures and grain sizes were collected from each outcrop. Polished thin sections were prepared for petrographic analysis, microstructural analysis, electron microprobe analysis, and in-situ microprobe dating. The general approach to *in-situ* monazite dating is summarized in Williams et al. (2006) and updated in Williams et al. (2017). Full-section compositional maps are collected early in the analytical process using the Cameca SX50 electron microprobe. For this study, maps were collected for Mg, K, Ca, Ce, and Zr. The Mg, K, and Ca maps show the distribution of the major silicate phases. Ce and Zr maps show the location of all monazite and zircon grains respectively (See Williams et al., 2006).

Next, high resolution maps are collected for a number of monazite grains (typically 20 or more) in the section. Maps for Y, Th, U, Ca, and one other element (Si, Nd, Gd, As, etc.) are collected. The maps are processed simultaneously such that intensities are comparable from grain map to grain map (Williams et al., 2006; 2017). It is particularly informative for high-resolution maps to be placed around the full-section image with links to the actual grain locations. This allows the zonation within a particular grain to be interpreted in the context of its textural and microstructural setting within the thin section. Important domain types are selected from the combined assemblage of grain maps; commonly between 3 and 6 domain types are present in a typical thin section. A dating strategy is developed whereby each domain type is sampled (dated) several times with preference given to grains where two or more domains can be sampled from the same grain.

Monazite dating was carried out on the Cameca Ultrachron electron microprobe at the University of Massachusetts. The instrument was specifically designed for trace-element analysis and geochronology (Jercinovic et al., 2008a, 2008b). The analytical protocol is described in Williams et al. (2017) and is briefly summarized here. For each compositionally-defined domain, a single background analysis is acquired first, followed by 6-8 peak measurements near the background location. Background intensities are determined using the "multipoint" method (Allaz et al., 2018); measurements are made in four to eight locations on either side of the peak position. The bremsstrahlung curve (background) is determined by regression of acceptable measurements and then the background is calculated at the peak position. One "date" is calculated for each domain. Uncertainty is calculated by propagating measurement and background errors through the age equation (Williams et al., 2006). Dates are typically shown as a single Gaussian probability distribution function for the dated domain.

Zircon U-Pb analyses were carried out at the Arizona Laserchron Laboratory. Analyses were made on bulk zircon separates and in-situ in thin section. Bulk analyses were carried out according to methods outlined in Gehrels et al., (2008); and (https://drive.google.com/file/d/0B9ezu34P5h8eTU9PaUczTGc5elk/view). Polished thin sections for in-situ analysis were first mapped for Zr (as described above) in order to locate all zircon crystals. Individual zircon grains were imaged by high-resolution backscattered electron imaging and then by cathodoluminesence imaging in order to select domains for dating. Polished sections were analyzed with either 10 or 15 µm laser beam size with standards mounted adjacent to the thin section. Data were reduced using procedures outlined in Gehrels et al., (2008).

METAMORPHIC CONDITIONS AND MELTING REACTIONS

Metamorphic assemblages from aluminous metasedimentary rocks are similar in all three localities. Most samples contain K-feldspar, garnet, quartz, biotite, sillimanite, +/- rutile, monazite, zircon, and apatite. Biotite is interpreted to be mainly a retrograde phase, but in some samples, some biotite was certainly present at peak conditions. Phase diagrams have been calculated by a number of workers for pelitic bulk compositions, and relationships for moderate-pressure granulites are very similar (Storm and Spear, 2005; White et al., 2007; Yakumchuk and Brown, 2014; Yakumchuk, 2017), see Figure 3.

The lack of peak biotite and plagioclase and the abundance of garnet and K-feldspar suggests that the following were important melting reactions.

$$Bt + Pl + Als + Qtz = Grt + Kfs + melt \quad (1)$$

$$Bt + Als + Qtz = Grt + Kfs + melt \quad (2)$$

Some initial melting may have occurred earlier associated with muscovite dehydration, but modeling suggests that the amount of melting (i.e. melt production) was probably limited (Storm and Spear, 2005; Yakumchuk and Brown, 2014). We suggest that the P-T conditions of metamorphism for these samples generally fall within the region shown on Figure 3.

Estimates of peak metamorphic temperatures and pressures are rather uniform, on the scale of kilometers, across the Adirondack Highlands (Bohlen et al., 1985; Spear and Markussen, 1997; Storm and Spear, 2005). All previous workers agree that peak conditions were on the order of 750 °C (or higher), 0.7-0.8 GPa in the central Adirondack Highlands. Bohlen et al. (1985) showed a concentric pattern of P's and T's and suggested that the pattern may reflect doming of preexisting isograds. However, a persistent question concerns the age of the metamorphism. Calculated conditions could represent late (ca. 1150 Ma) Shawinigan, Ottawan (ca. 1090), or late Ottawan (ca. 1050-1030) metamorphism, and it is likely that a combination of these events resulted in the preserved assemblages and compositions.

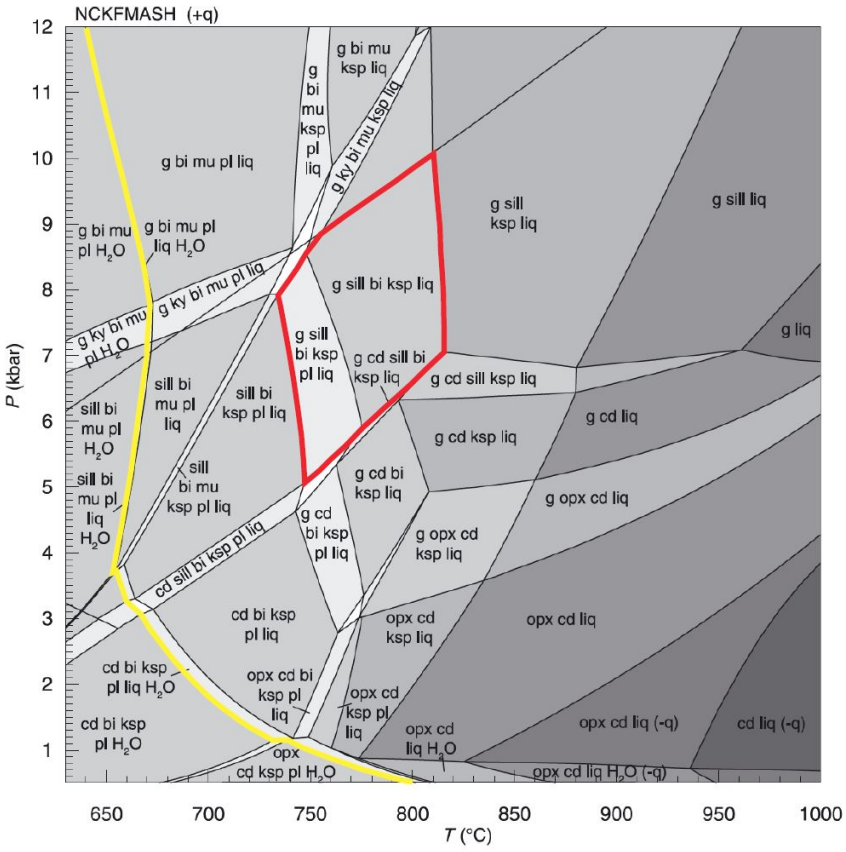

Figure 3. Model phase diagram for a theoretical pelitic (Al-rich shale). From White et al., (2007). Rocks from this study are interpreted to have been metamorphosed within the area outlined in red.

RESULTS

Locality-1: Rt. 8 Migmatites, Hague, NY

Samples have been investigated from three separate outcrops along Rt. 8, west of Hague New York (Williams et al., in review). From west to east, these are Treadway Mtn, Swede Pond, and Elephant rock (Fig. 1). Figure 4 shows full-thin-section compositional maps from the samples. All three samples contain the common assemblage: biotite, garnet, quartz, sillimanite, apatite, rutile, zircon, and monazite. However, major differences occur in the mode, composition and distribution of feldspar and also in the mode and distribution of biotite.

Sample 16TG-154 (Swede Pond) contains no plagioclase, only K-feldspar (Fig. 4a,b). The K-feldspar is extremely abundant making up much of the matrix of the sample (Fig. 4b). The complete lack of plagioclase and prograde biotite in this sample suggests that Reaction-1 was exceeded. That is, the sample underwent extensive bt-dehydration melting. Also, the lack of plagioclase suggests that the melting reaction was not reversed, i.e. the melt did not crystalize within this sample. Instead, we suggest that a significant portion of the melt component was removed or segregated from the local (residual) rock.

Samples 16TG-151 (Treadway Mtn.) and 16TG-150 (Elephant Rock) contain both plagioclase and K-feldspar, but have distinctly different textures. 16TG-150 contains coarse grained K-feldspar and plagioclase, particularly in the shadows of large garnet porphyroblasts (Fig. 4 d,e). Leucosome layers with annealed or undeformed feldspars wrap around the garnet porphyroblasts. Samples from locality151 (Treadway Mtn.) contain dispersed, fine to medium grained, plagioclase and K-feldspar (Fig. 4 g,h). Both of these samples are interpreted to have undergone melting by a similar bt-dehydration reaction, but at least some leucosome crystalized locally, that is, the melting reaction was at least partially reversed in these samples. The differences between the three samples may reflect subtle differences in the original bulk composition, but they may also involve different amounts of strain partitioning that, in turn, helped to facilitate melt segregation/removal (see below).

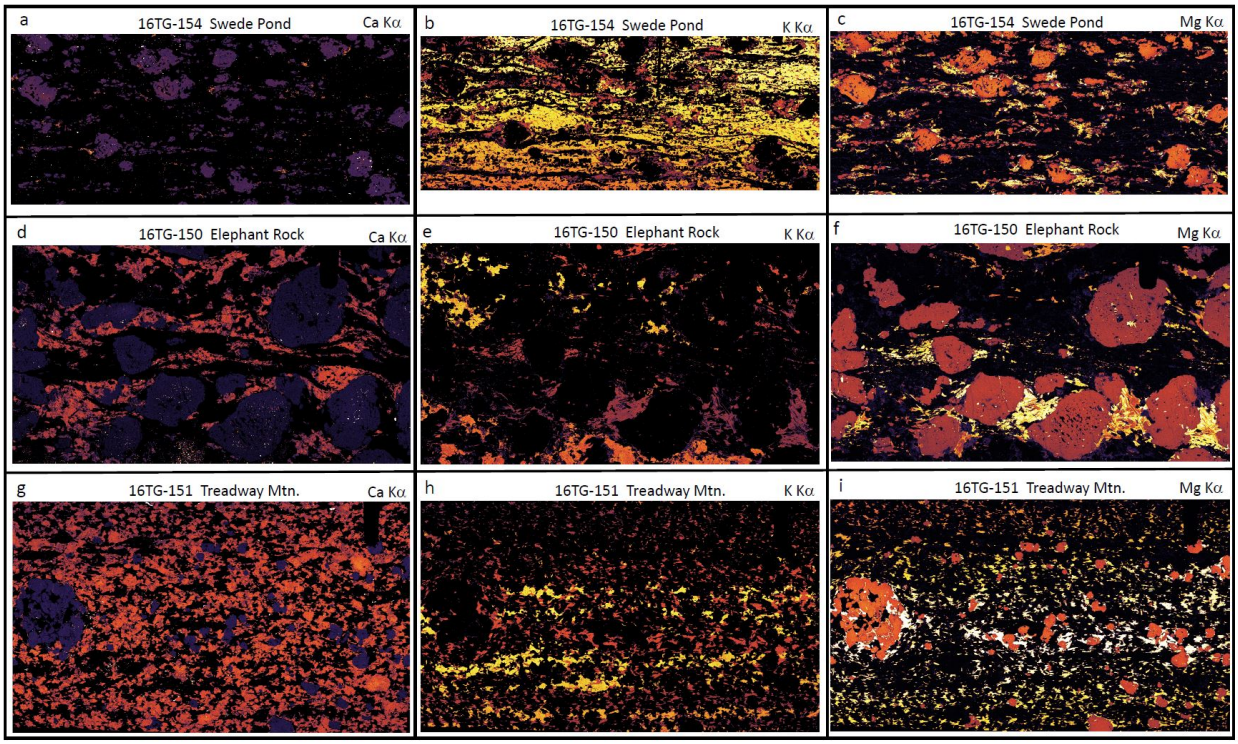

Figure 4. Compositional maps for samples from Locality-1, Rt. 8, Hague, NY. Each map covers a full-thin section for the specified elements. Brighter colors represent greater abundance of the element. See text for discussion.

Monazite Data Figure 5 is a summary of monazite data from the three Rt.8 outcrops discussed above. As noted, each probability distribution represents one monazite date, obtained from one compositional domain in a single monazite grain as delineated by grain mapping. Color codes show the main domain types (i.e. core, outer

core, main, rim). Details about the analyses, monazite compositions, and interpretation are presented in Williams et al., in review). Typical uncertainties (2σ) range from ca. 4 m.y. to very rarely greater than 20 m.y.

Note: We use the term "date" to refer to the results of the age equation using measured U-Th-Pb values. The term "age" refers to the interpretation of a date such as the age of a particular rock or process.

Figure 5 d,e,f show Y-content in monazite vs. calculated date for the three samples. Horizontal scales are equal so that each point in the composition plot corresponds to one probability distribution. Arrows connect cores and rims when analyses come from the same grain. Y is strongly partitioned into garnet and has been used in many studies to link monazite growth with garnet growth and breakdown (see references in Williams et al., 2007). The characteristic 'U-shaped' profile (Fig. 5d) is interpreted to result from significant garnet growth (decreasing Y) and garnet breakdown (increasing Y).

Figures 5 g,h,i show U content in monazite vs. calculated date. Partitioning data from Stepanov et al. (2012) indicate that the actinides (U, Th) have positive monazite/melt fractionation, but U has a significantly lower ratio than Th and most REEs. During partial melting U and other trace and REEs will be partitioned from the whole rock into melt. Monazite in equilibrium with the melt will be depleted in uranium relative the other actinides or REEs, and monazite in restite will be expected to equilibrate with the lower bulk-rock uranium abundance. Thus, a decrease in U in monazite is interpreted to result from partial melting of the sample. A reduction in U synchronous with a Y and HREE reduction is consistent with melting by reactions 1 and 2 where garnet is produced as a peritectic phase during melting. If the U content of monazite remains low during cooling or subsequent thermo-tectonic events, we suggest that a significant component of the melt was removed from the local system.

Interpretation – Locality-1. The three samples/localities summarized here are similar in outward appearance. They are all garnet-rich migmatitic gray gneisses. But compositional maps and the monazite record suggest that they have very different petrologic, microstructural, and petrotectonic histories, especially with regard to melting and melt loss. Sample 16TG-154 (Swede Pond) experienced significant melting at ca. 1160-1150 Ma and judging by the dominance of garnet and K-feldspar and lack of plagioclase, the sample shows little evidence for back reaction and melt crystallization. Much of the partial melt in this sample is interpreted to have left the system. The monazite record suggests that little garnet growth or melting occurred during the Ottawan orogeny (ca. 1090-1050 Ma).

Sample 16TG-150 (Elephant Rock) contains a significant amount of plagioclase in addition to K-feldspar, garnet, biotite and quartz. One characteristic feature of this sample is the coarse segregation of minerals, especially feldspar and biotite into distinct layers. Like sample 16TG-154, the monazite record suggests that significant melting occurred at ca. 1150 Ma and that little if any melting or garnet growth occurred at ca. 1050 Ma. However, unlike 16TG-154 (Swede Pond), U does not show a significant decrease after 1150 Ma. Although the leucosome was segregated into distinct layers, any U partitioned into the melt was apparently released back into the rock on crystallization and was thus, available for incorporation into later monazite. We suggest that, even though the components were present for melting, the segregation of minerals, especially feldspars and biotite at the end of the early melting event, may have left the sample relatively infertile for subsequent melting (Williams et al., in review).

Sample 16TG-151 (Treadway Mtn.) shows evidence for garnet growth and melting at 1150 Ma and also at 1050 Ma. Y and HREEs decrease in two sharp steps, one at ca. 1150 Ma and one at ca. 1050 Ma. This sample also has by far the greatest volume of ca. 1050 monazite domains, interpreted to have grown during melt crystallization. Because the U-content remains relatively high and constant from the ca. 1150 Ma to ca. 1050 Ma (Fig. 5), the 1150 melt component is interpreted to have remained dispersed within the rock, releasing U back to monazite on crystallization. Consequently, this sample was more fertile for melting during the Ottawan Orogeny.

All three samples investigated in this study have a strong, shallowly-dipping foliation and weak (if any) lineation. It would be tempting to correlate this fabric from locality to locality in the three closely-spaced localities. However, based on the fabric and monazite record, samples 16TG-150 and 154 largely preserve their 1150 Ma migmatitic fabric while the fabric in 16TG-151 was reactivated at 1050 Ma. The Shawinigan Orogeny apparently involved crustal thickening culminating in partial melting at ca. 1160-1150 Ma (Rivers, 2008; McLelland et al., 2013). The associated melt weakening is interpreted to have led to the subhorizontal migmatitic fabric preserved in samples 150 and 154. Both samples do have subtle evidence for west-directed shearing. We suggest that at ca. 1050 Ma localized melting in certain fertile localities led to a second phase of melt weakening and fabric development roughly parallel to the preexisting fabric.

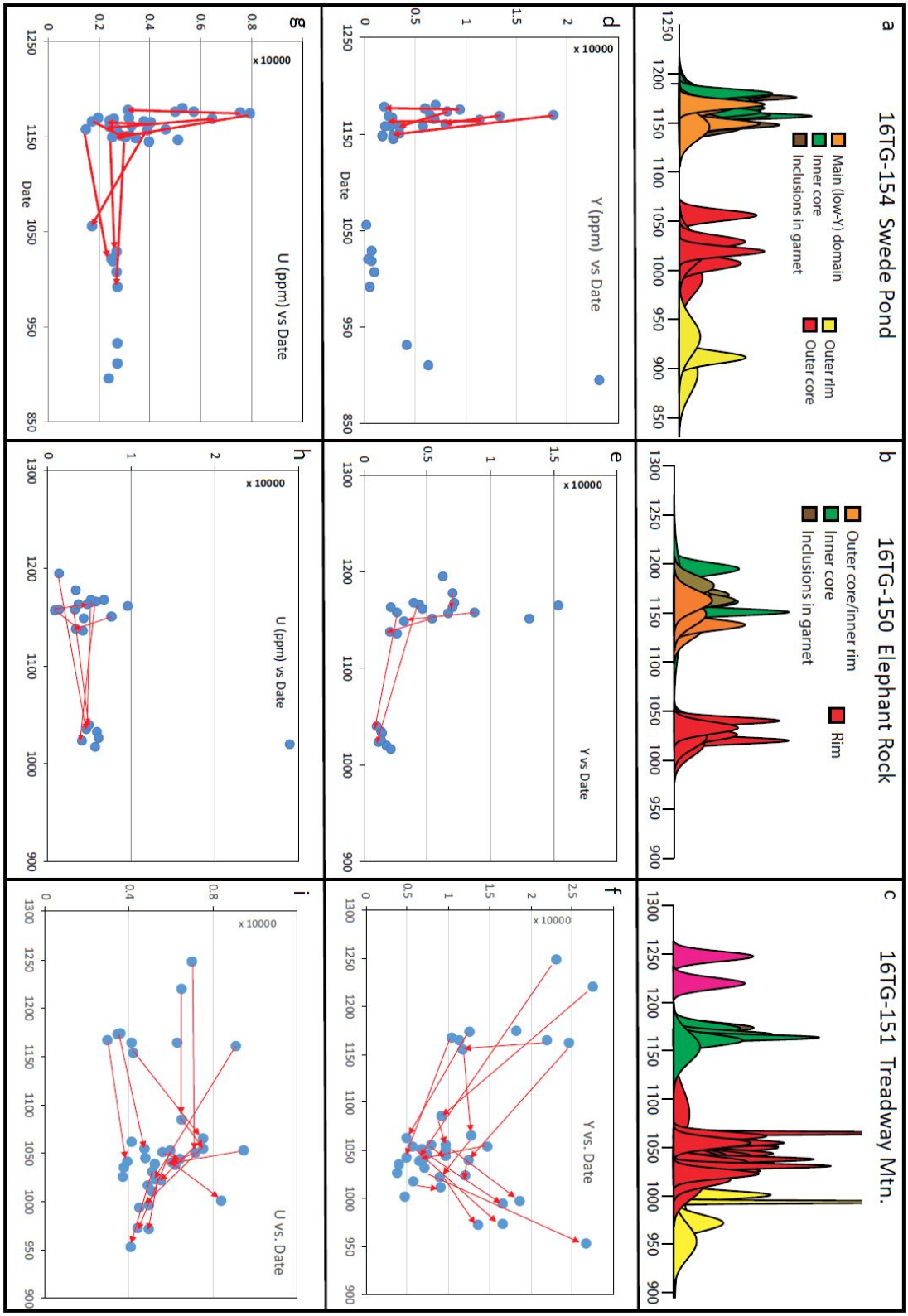

Figure 5. Monazite-date-composition relationships for samples from three outcrops along Rt. 8, Hague, NY. See text for discussion.

Locality-2 Dresden Station

The Dresden Station outcrops have been the focus of a number of publications and field excursions. McLelland et al. (1988a) cite evidence from this outcrop to show that there were multiple phases of metamorphism recorded by the rocks in the Adirondack Mountains. A sharp contact between garnet-sillimanite gneiss and a coronitic metagabbro is well-exposed. The gneiss is a garnet-sillimanite-plagioclase-K-feldspar-quartz gneiss with a small amount of biotite, commonly referred to as khondalite. The garnet-sillimanite gneiss is penetratively deformed with a well-developed foliation and a lineation that plunges gently to the east. Much of the metagabbro is undeformed and a coarsely crystalline texture is preserved throughout portions of the unit. The gabbro is finely crystalline right at the contact with the gneiss and appears to get more coarsely crystalline towards the interior of the body suggesting a chilled margin formed at the contact between the gabbro and the gneiss. The foliation in the khondalite gneiss is sharply cut by the contact between the gneiss and the metagabbro. This contact relationship suggests that the gneiss was deformed and metamorphosed prior to the intrusion of the gabbro (McLelland et al., 1988a). McLelland et al. (1988b) report a U-Pb zircon, multigrain age of 1144 ± 7 Ma for the metagabbro. This is interpreted as an igneous crystallization age and is consistent with the gabbro belonging to the AMCG suite.

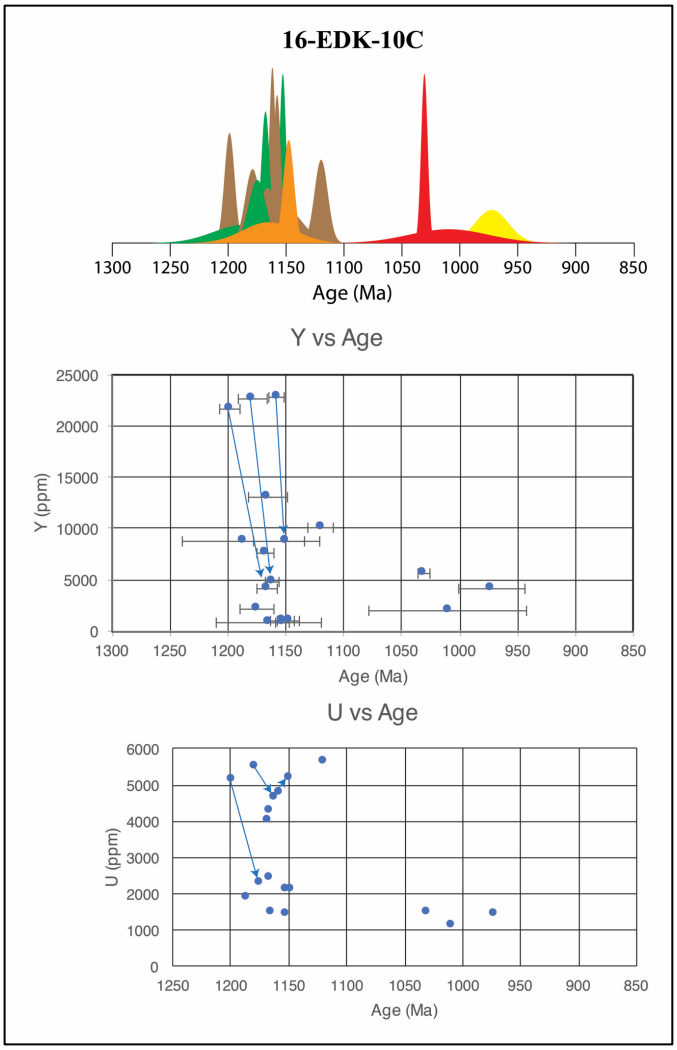

Figure 6. Monazite date-composition relationships from sample EDK-09-10C, Dresden Station khondalite. See text for discussion.

We analyzed monazite from several thin sections of the garnet-sillimanite gneisses (Fig. 6). The data broadly suggest three distinct periods of monazite growth. The oldest population has a weighted mean of 1179 ± 9 Ma. We suggest that this is the age of prograde metamorphism and fabric development in the garnet sillimanite gneisses. The next population yielded dates that cluster around 1151 Ma. We hypothesize that this represents a period of monazite growth driven by a thermal perturbation resulting from the intrusion of the AMCG gabbroic rocks. The date correlates well with the reported age of the gabbro at this outcrop. The third population yields dates of 1030 Ma or younger. These are too young to correlate with the proposed timing of the peak of the Ottawan Orogeny (~1090-1050 Ma). Instead we interpret this generation to represent the period of post-Ottawan decompression and uplift.

The following model is consistent with the field observations and data from this outcrop. The mineral assemblage and the fabric in the garnet-sillimanite gneisses formed during the Shawinigan Orogeny. The gabbro was emplaced at approximately 1150 Ma, after the prominent fabric developed in the gneisses. This time frame is consistent with both the monazite ages from the gneisses and the multigrain age from the gabbro. Following the emplacement of the gabbro there was another period of deformation and metamorphism. This is when the nearby AMCG rocks were deformed and metamorphosed. This is also when the coronitic texture developed in the metagabbro. This requires in influx of an H_2O–bearing fluid. Unlike the nearby rocks, the coronitic metagabbro was not pervasively deformed at this time nor did any new monazite grow in the garnet-sillimanite gneiss. Perhaps strain was partitioned around this outcrop and the lack of strain resulted in little recrystallization in the largely anhydrous garnet-sillimanite gneisses. The 1020 Ma and younger monazite ages in the garnet-sillimanite gneisses record monazite growth during post Ottawan extensional collapse.

Locality-3: Migmatites of the East Adirondack Shear Zone

Outcrops of garnet, sillimanite, biotite, quartz, feldspar gray gneisses with abundant leucosome layers are common along Rt. 22 south of Whitehall, NY. Locality-3 was also the focus of a study by Wong et al. (2012) and of one M.S. thesis (Suarez et al., 2017; Suarez, 2018). The outcrop contains interlayered garnet-biotite-sillimanite gneisses with greenish calcsilicate lithologies. The well exposed foliation surfaces of the gneisses commonly have well-lineated, coarsely crystalline sillimanite. The lineation is gently plunging to the southeast on an east-dipping foliation. Variations in the amount of biotite, garnet, and the proportions of feldspars are interpreted to reflect variation in the amount of melting by Reaction 1 and 2 and also in the amount of melt segregation and melt loss.

Wong et al. (2012) investigated deformational fabrics in this outcrop and in granite-bearing outcrops immediately to the south. They report a U-Pb zircon date of the granite of ca. 1140 Ma. This date suggests that the granite is part of the AMCG suite and was emplaced towards the end or after the Shawinigan Orogeny. Following this reasoning, they suggest that most of the strain in the rock is therefore related to Ottawan compression or post Ottawan extension. They examined the asymmetric K-feldspar porphyroclasts as kinematic indicators to document shear sense. Although they found some porphyroclasts that suggested top to the west, thrust sense motion and others that suggest top to the east, normal-sense motion, those that indicate top to the east movement were more abundant by a ratio 3:1. From this they concluded that this rock experienced both shortening and extension, but the extensional event was younger and overprinted the shortening event.

Geochronology. In-situ monazite analyses have been carried out as part of this work (Suarez et al., 2017) and also as part of the Wong et al (2012) study. Six distinct compositional populations (generations) have been recognized in the migmatitic metasedimentary samples: 1178 Ma, 1139 Ma, 1064 Ma, 1049 Ma, 1030 Ma, and ca. 1000 Ma (Fig. 7); see also Suarez et al. (2017). Uncertainties are on the order of 10-20m.y. (2σ). There is a distinct drop in Y and HREE between the ca. 1140 and ca. 1060 populations. An additional decrease occurs between 1064 and 1049 Ma. Uranium also shows decreases in the 1060-1050 Ma range. Although work is still underway, there is little evidence in these rocks for significant melting at ca. 1150 Ma. The data are consistent with the dominant melting event to have occurred at ca. 1060 Ma. The lowest Y and REE and U contents are associated with the ca. 1050 Ma population, suggesting that garnet growth and additional melting continued to this time (Fig. 7). It is possible that there was one prolonged melting event or alternatively melting may have occurred during the culmination of Ottawan shortening (1090-1060 Ma) and a second event associated with post Ottawan extension and intrusion of the Lyon Mountain granite (ca. 1050 Ma).

The 1030 Ma population is interpreted to represent shearing associated with the East Adirondack shear zone (Wong et al., 2012). Y and HREE contents increase dramatically after 1050 Ma, probably reflecting garnet break-down during exhumation (Fig. 7). The relatively high-Y overgrowths on monazite grains are commonly located along the foliation and in extensional quadrants of the grains further supporting the connection between this monazite generation, extensional shearing, and exhumation (see Wong et al., 2012). Based on the extremely low Th-content, the youngest population (ca. 1000 Ma) is interpreted to represent monazite associated with fluid infiltration and hydrothermal alteration events.

Monazite is present in thin leucosome layers within the gray migmatitic gneiss and also in thicker leucosome layers in the outcrop (Fig. 8). Monazite from a thin (~ 1 cm) leucosome layer yielded dates 1050 Ma and younger. Because monazite is expected to dissolve into partial melt, i.e. most partial melts are undersaturated in monazite components (Kelsey et al. 2008; Yakymchuk and Brown 2014; Harley and Nandakumar, 2014), we interpret the ca.1050 date to be the time of crystallization of this leucosome layer. Monazite from larger, more discrete leucosomes also yielded ca. 1050 Ma dates. However, these monazite grains have much greater U-content than the gray gneiss or the thin leucosome. We suspect that these leucosomes represent injections of external partial melts that have fractionated and evolved to higher U contents.

We have carried out in-situ and bulk zircon (U-Pb) analysis of some rocks from this outcrop. Analyses were done by Laser-ICP-MS at the Arizona Laserchron Laboratory. Bulk separates from gray gneiss yielded only ca. 1050 dates but in-situ samples of the gray gneiss yielded both ca. 1150 and ca. 1050 dates (Fig. 7, 8). We suspect that this reflects a sampling bias where only the larger zircon grains were recovered during mineral separation and these are dominated by the younger populations. An analysis of a zircon separate from the thin leucosome layer from which monazite was also analyzed, yielded both ~1150 and ~1050 dates (Fig. 8). We suspect that the older dates represent inherited zircon incorporated into the partial melt from the gray gneiss (see Suarez et al., 2017).

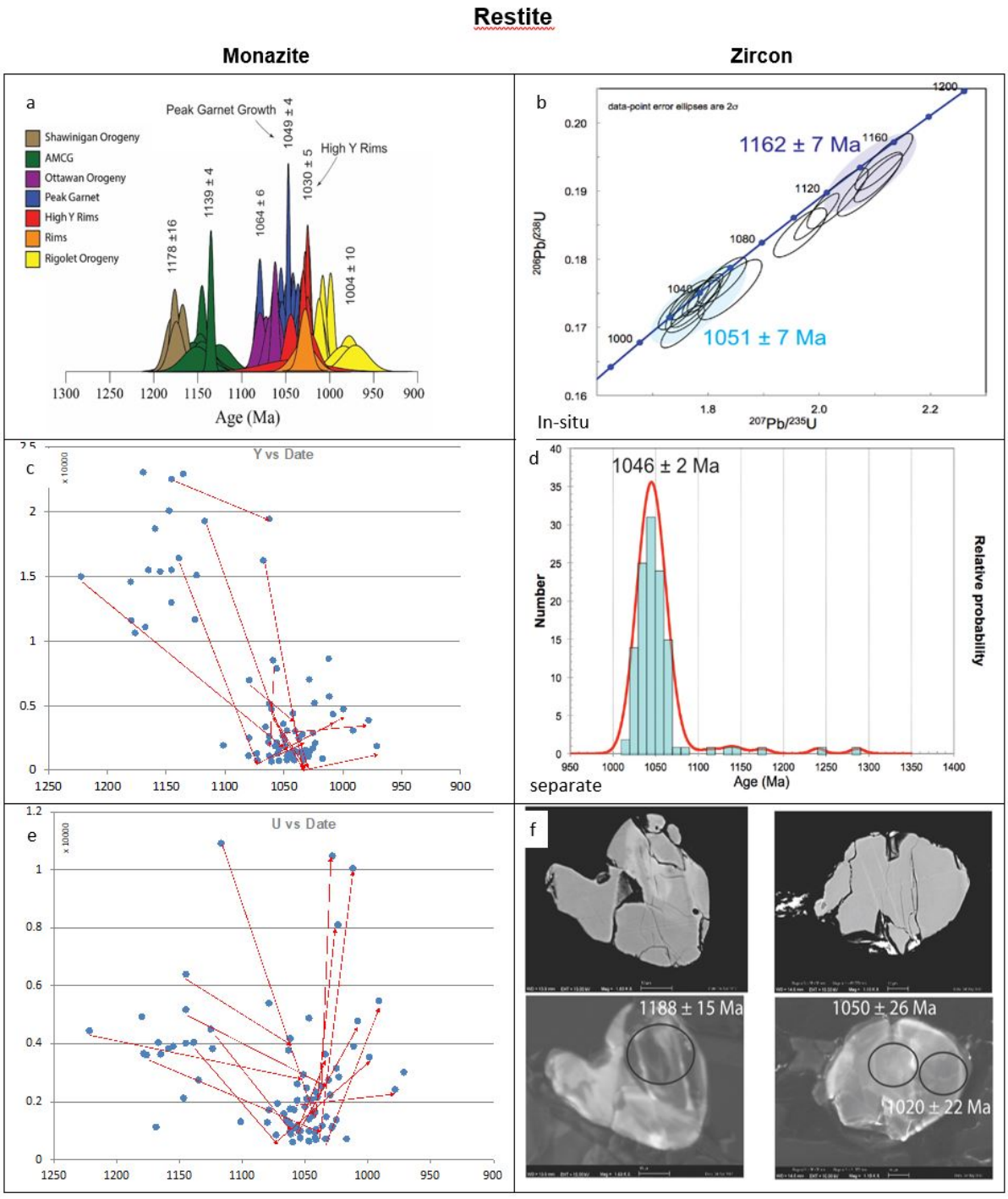

Figure 7. Monazite and zircon date-composition relationships from the restite layer, Rt. 22, south of Whitehall, NY. See text for details. A) Monazite dates for the restite. The results show six distinct populations at 1178, 1139, 1064, 1049, 1030, and 1004 Ma. B) Concordia diagram from in-situ restite zircon with two major populations at 1162 and 1051 Ma. C) Monazite yttrium composition vs date. The sharp decrease in Y in the 1050 Ma population suggests significant garnet growth. D) Zircon probability density plot for the restite mineral separate, showing one population at 1046 ± 2 Ma. E) Monazite uranium composition vs date. The U decreases at 1050 Ma and increases at 1030 Ma, suggesting melt loss and hydrothermal alteration, respectively. F) BSE and CL images of in-situ zircon with associated dates.

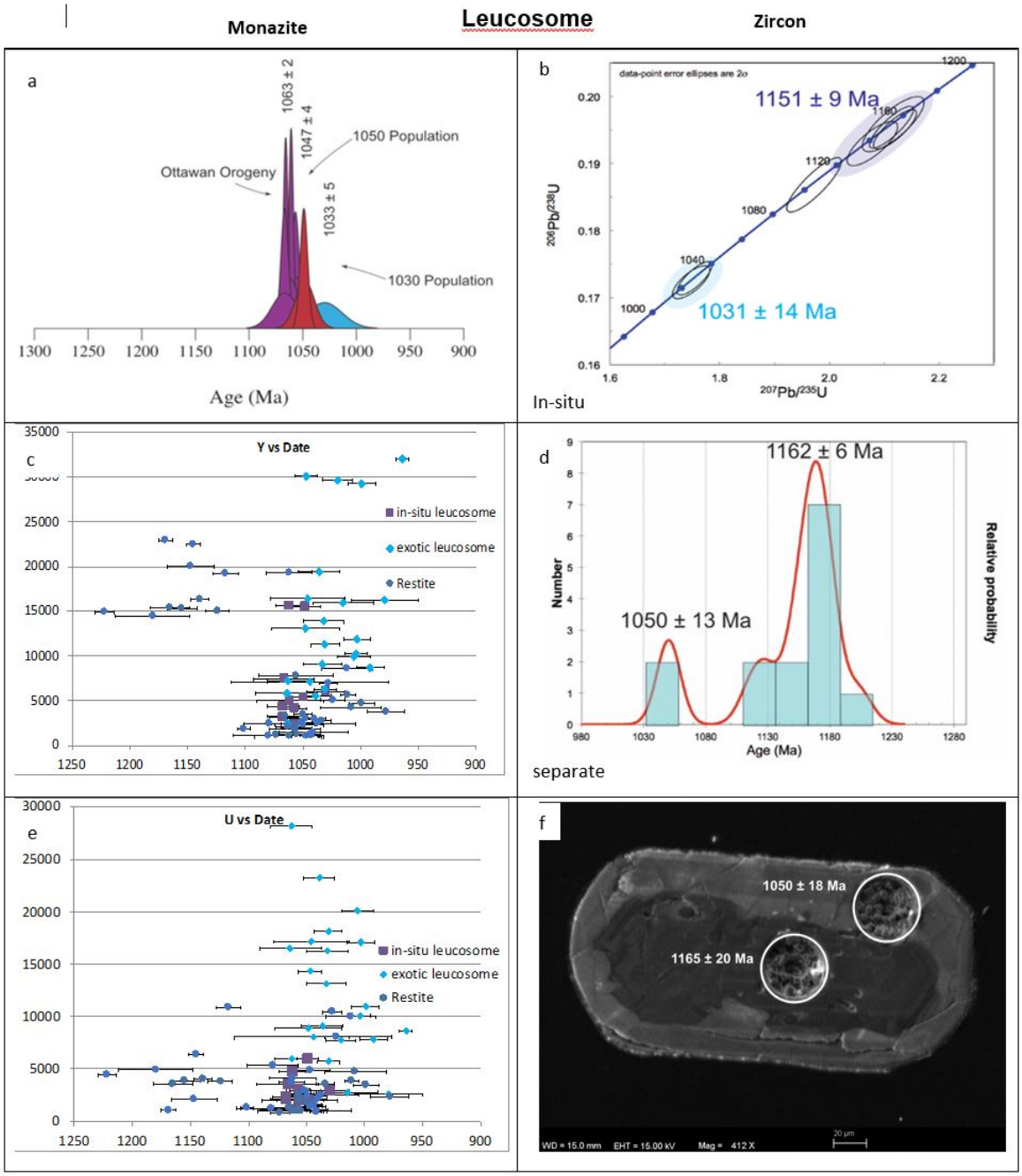

Figure 8. Monazite and zircon date-composition relationships from a leucosome layer from the same sample as Figure-7. See text for details. A) Monazite dates for the leucosome layer showing three distinct populations: 1063, 1047, and 1030 Ma. B) Concordia diagram from the in-situ leucosome zircon with populations at 1151 and 1031 Ma. C) Monazite yttrium composition vs date for in-situ leucosome, exotic leucosome and restite. The exotic leucosome has the highest Y values. D) Zircon probability density plot for the leucosome mineral separate, showing two populations: 1162 ± 6 Ma and 1050 ± 13 Ma. E) Monazite uranium vs. date for in-situ leucosome, exotic leucosome and restite. The exotic leucosome has significantly higher uranium. F) Cathodoluminescence photograph of the zircon with a 1165 ± 20 Ma core and a 1050 ± 18 Ma rim. The 1050 Ma rim date is interpreted to be the age of the leucosome.

DISCUSSION

At least three regional tectonothermal events have been recognized in the Adirondack Highlands: the (1190-1140 Ma) Shawinigan orogeny, the (1090-1020 Ma) Ottawan orogeny, including post-Ottawan extension, and the poorly understood (1010-980 Ma) Rigolet stage/orogeny (Rivers, 2008; McLelland et al., 2013; Chiarenzelli et al., 2017). One of the major challenges for interpreting the tectonic history of the region involves placing fabrics, textures, and metamorphic assemblages into the context of these events. This is particularly true of the Shawinigan and Ottawan orogenies, which have both been interpreted to involve granulite facies metamorphism, partial melting, and penetrative deformation (Heumann et al., 2006; Bickford et al., 2008). Monazite and zircon domains from this study have yielded dates in each of the main age ranges including abundant data that span the (ca. 1160-1140 Ma) time of AMGC plutonism. Compositional mapping and composition-date relationships provide a number of insights into the significance of these generations and into the tectonic history of the region in general.

In the following discussion, dates and interpreted ages will be presented mainly without uncertainties for brevity and clarity. Errors on most monazite dates are on the order of 10-20 m.y. and the two major granulite facies events are separated by approximately 100 m.y. (Shawinigan: 1190-1140 Ma vs. Ottawan: 1090-1020 Ma). For the following discussion, the Shawinigan/AMCG event will be considered to be ca. 1150 Ma and the Ottawan event will be considered to be ca. 1050 Ma.

Timing of Partial Melting

Shawinigan/AMCG Melting. Samples from all three localities investigated here have Shawinigan/AMCG monazite domains. These tend to occur as cores in zoned monazite grains or as monazite inclusions in garnet. Localities 1 and 2 show a dramatic decrease in Y, HREEs and U at approximately 1160-1150 Ma. In agreement with Heumann et al. (2006) and Bickford et al. (2008), these data are taken to indicate a significant period of partial melting and garnet growth. Importantly, this overlaps with the age of AMGC plutonism, near the end of the Shawinigan orogeny. We suggest that heating from AMGC intrusions and associated gabbroic intrusions may have contributed to the high temperature of metamorphism and may help to explain the abundance of migmatite in paragneiss across the Adirondack Highlands. There is little evidence for Shawinigan melting in samples from Locality-3. We suspect that temperatures were not high enough for extensive biotite-dehydration melting in this locality. This may be due to variations in the depth of exposure and thus temperature (i.e. Bohlen et al., 1985), but it may also reflect the greater distance to high-T, AMCG gabbro and anorthosite.

Samples from Swede Pond (Locality-1) contain the silicate assemblage Bt (retrograde)-Sil-Grt-Ksp-Qtz and are interpreted to reflect the almost complete progression of Reactions 1 and 2. That is, biotite and plagioclase were exhausted, and the assemblage is dominated by the solid products of melting (garnet and K-feldspar). The lack of plagioclase-bearing (leucosome) domains and the stability of the product assemblage suggests that partial melt was lost from the local assemblage. Other samples do contain biotite and plagioclase, either dispersed or localized in discrete layers. Importantly, many of these samples do not show the distinct decrease in U that is seen in the K-feldspar dominated samples. We suspect that, at least in some locations, a portion of the Shawinigan-AMCG partial melt did crystallize locally, producing plagioclase and biotite and maintaining high U-levels in monazite. However, the abundance of garnet suggests that some melt was also lost. If not, one would expect that much of the garnet produced during melting would be consumed during melt crystallization (White et al., 2002).

Ottawan Melting. The Ottawan orogeny is interpreted to have occurred in the range 1090-1020 Ma, based on regional constraints (Rivers, 2008). However, locally, some workers would break the event into an early prograde or peak phase (1090- ca.1070 Ma) and a later extensional phase (1070-1020 Ma) (Wong et al., 2012; Chiarenzelli et al., 2017). Peak conditions are estimated to have been in the granulite facies, perhaps similar to those in the Shawinigan orogeny (Spear and Markussen, 1997; Peck et al., 2018). Samples from Swede pond, at Locality-1, and all samples form Locality-2 (Dresden Station) have yielded essentially no monazite grains/domains with dates in the 1090-1060 range, and there is little evidence for new melting in these samples. Y and HREEs were depleted at 1150 Ma. U shows no additional change after approximately 1150 Ma.

Samples from Locality-3 and some samples from Locality-1 (i.e. Treadway Mountain) are very different. Numerous monazite domains and whole grains yielded dates in the 1090-1050 Ma range, especially between 1060 and 1050, the presumed prograde/peak phase of the Ottawan event. Importantly, numerous grains show a core-to-rim drop in Y, HREEs, and U at this time. We interpret this to indicate new garnet growth and a new phase of partial melting by reactions 1 and/or 2. So far, garnet compositional mapping and quantitative traverses have not definitively shown two distinct garnet compositions or textures. This may not be surprising because the Ottawan

event is interpreted to have involved high temperatures (>800 C) (Spear and Markussen, 1997) and thus, rapid diffusion. Also, the operation of similar reactions at similar grades may have produced similar garnet compositions.

Retrograde Metamorphism

Monazite examined in this study, as well as monazite from around the eastern Adirondack Mountains, shows evidence of retrograde metamorphism starting at approximately 1030 Ma. Y and HREEs in monazite increase significantly in monazite domains younger than ca. 1050 Ma. The increases are interpreted to reflect breakdown of garnet and release of HREES and Y. The Y- and HREE enriched domains typically occur as narrow rims, and are never present on grains completely enclosed in garnet.

Several samples are characterized by decreasing Th in monazite domains younger than approximately 1000 Ma. This seems somewhat contradictory to the interpretation that Th is strongly partitioned into monazite relative to melt of other major minerals (Stepanov et al,2012; and see above). However, there is some evidence that Th may be removed from monazite during fluid alteration by a dissolution reprecipitation mechanism (Putnis and Austrheim, 2010; Harlov and Hetherington, 2010; Williams et al., 2011). Several of the low-Th domains show textural evidence of alteration rather than overgrowth, for example, irregular low-Th domain boundaries cutting earlier domain boundaries (see Williams et al., 2011). Dissolution reprecipitation may be particularly effective in the presence of Na-bearing fluids (Harlov and Hetherington, 2010; Harlov et al., 2011). This would be consistent with the characteristic Na-metasomatism associated with late iron mineralization in the eastern Adirondacks (Valley et al., 2010; 2011). We tentatively suggest that this late depleted Th signature may be a signal of the late hydrothermal phase of evolution of the Adirondack Highlands.

It is interesting that, although there is widespread preservation of early, ca. 1150 Ma and older, monazite cores, there are no high-Y/REE rim domains of this late-Shawinigan age. Exhumation/collapse has been interpreted to have occurred soon after the Shawinigan orogeny (Rivers, 2008; McLelland, 2013) and would be required if the 1155 Ma Marcy anorthosite was emplaced into shallow crust (Valley and O'Neill, 1982). However, the fact that monazite in these samples is very sensitive to decompression and garnet break-down after 1050 Ma, but there is little evidence for garnet break-down after 1150 Ma suggests that there may have been less post-Shawinigan decompression in the Adirondack Highlands than previously thought.

Timing of Deformation

Textural evidence suggests that one major gneiss-forming deformational event occurred synchronous with partial melting at ca. 1160-1150 Ma (Williams et al., in review). K-feldspar-rich leucosomes from Locality-1 show evidence for pooling of leucosome in garnet shadows. Also, imbricated garnet that is wrapped by annealed K-feldspar suggests flow of garnet crystals during leucosome formation (Williams et al., in review). The ca. 1150 Ma monazite domains are distinctly aligned in the main migmatite layering. These domains probably reflect local melt crystallization, and they support interpretation of syn-melting deformation. Older monazite inclusions in garnet are not aligned in the migmatitic fabric.

Mineral lineations and kinematic indicators are poorly developed in many of the migmatite samples interpreted to have formed in the ca. 1150 event. This is in distinct contrast to a meta-quartzite at Locality-1, which has a strong mineral lineation (see Williams et al., in review). We suspect that the melt-weakened rocks at ca. 1150 Ma were not particularly amenable to lineation formation, but it is possible that some annealing occurred during later (Ottawan) orogenesis. Pooling of leucosome, possible imbrication of garnet, and subtle shear bands provide a low-confidence top-west sense of shear. This is opposite of the sense interpreted for the (ca. 1050-1030 Ma) East Adirondack shear system along the eastern edge of the uplift (Wong et al., 2012) and may characterize Shawinigan deformation in this area.

Late-stage monazite domains (>1050 Ma) have little preferred orientation in Localities 1 and 2. However, ca. 1050-1030 monazite overgrowths from Locality-3 are distinctly oriented along the SE-plunging mineral lineation. In fact, some overgrowths form sigma-tails consistent with top-east normal shearing (Wong et al., 2012). Locality-3 occurs within the region that Wong et al (2012) interpreted to be part of the East Adirondack shear zone, related to orogenic collapse following the Ottawan orogeny. Interestingly, these rocks also have some of the strongest mineral lineations of any of the migmatitic gray gneisses sampled. We suggest that the high temperatures and presence of partial melt may have contributed to weakening and localization in the East Adirondack shear zone, but shearing may have outlasted melting leading to the development of a stronger lineation due to solid state deformation. Late-stage, decompression-related monazite overgrowths are present in all sampled localities, but the

lack of alignment of the overgrowths suggests that the other two localities were not specifically located within a collapse-related structure.

CONCLUSIONS

Partial melting can play a key role in the tectonic history of orogenic belts. Melting events can lead to weakening and thus, deformation of the crust and strengthening again when the melts crystallize. In addition, melting events record thermal perturbations that can have large-scale geodynamic significance. It is critical to illuminate the timing of melting and the relationship to deformation events and other tectonic events both before and after anataxis. Monazite can be a powerful tool for constraining the timing of metamorphism, melting, melt crystallization, and deformation.

Rocks from the three sample localities summarized here are similar in outward appearance, they are all garnet-rich migmatitic gray gneisses. However, compositional maps and the monazite record suggest that they have different petrologic, microstructural, and petrotectonic histories, especially with regard to melting and melt loss. All samples show evidence of monazite growth ca. 1150 Ma, but only localities 1 and 2 experienced significant melting. Judging by the abundance of garnet and K-feldspar some partial melt was lost from most rocks. Rocks in Locality-3 did not melt significantly during this early event perhaps because temperatures were lower near the margin of the present Adirondack dome and farther away from AMGC rocks.

The degree of partial melting and garnet growth during the Ottawan orogeny (ca. 1090-1050 Ma) was highly variable from locality to locality and, to some degree, from sample to sample. Although there is no evidence for melting or new garnet growth at Swede Mountain (Locality-1) or at Dresden Station (Locality-2), there is strong evidence for two periods of melting, Shawinigan and Ottawan, at Treadway Mtn. (Locality-1). Rocks at Locality-3 apparently underwent their first melting event during the Ottawan orogeny. These rocks have by far the greatest volume of ca. 1050 monazite domains, interpreted to have grown during melt crystallization.

A full explanation of the differing behavior must await additional analysis and more samples. Original bulk compositional differences probably played a role in controlling the degree of melting, especially at ca. 1160-1150 Ma. However, the dynamics of melt segregation and removal may have also played a role (see Williams et al, in review). We suggest that a significant proportion of melt at Localities 1 and 2 was removed and either lost from the system or segregated into distinct compositional layers. This apparently left these rocks relatively infertile for melting during the younger thermotectonic event. Rocks from Treadway Mountain may have undergone less melting during the earlier event, but importantly, it seems likely that any melt component remained dispersed in the rock producing a finer-grained, more homogeneous texture. After crystallization, the melt and restite components were more finely and evenly distributed, leaving these rocks more fertile for the second melting event. The rocks at Locality-3 were apparently fertile for melting at 1150 Ma, but did not melt, probably because metamorphic conditions were not high enough for significant biotite dehydration melting. These rocks were fully fertile for melting under Ottawan high-T granulite facies conditions.

All three localities investigated in this study have a strong, shallowly-dipping foliation. It would be tempting to correlate this fabric from locality to locality. However, based on the fabric and monazite record, deformational fabrics in gneisses from Locality-2 and parts of Locality-1 formed during the Shawinigan orogeny, while the fabrics at Treadway Mountain and Locality-3 formed or were reactivated at 1050 Ma. One would hope to be able to map, in the field, the effects of Shawinigan vs. Ottawan metamorphism and the effects of Shawinigan vs. Ottawan deformation. As noted earlier, the three localities investigated here are extremely similar in terms of outcrop appearance, fabrics and kinematics. However, some samples experienced Shawinigan melting and deformation, some record mainly Ottawan melting and deformation, and some record both events. At least for these gray gneisses, compositional mapping, detailed monazite analysis, and the integration of results from multiple samples is necessary to extract the full history.

ROAD LOG and FIELD GUIDE

Goals: The main goals of this trip are to look at and discuss migmatitic paragneisses (partially melted meta-sedimentary rocks) in the Adirondack Highlands. We will focus on three main localities, although several other outcrops may be visited in passing. Rocks from each of the three main localities are similar in appearance. They are gray, garnet-rich gneisses. However, recent monazite studies suggest that they may have very different histories. They may have been melted at different times, in different tectonic settings, at with different amounts of deformation.

Logistics: The trip will have two starting points. Some vans and cars will leave from the Fort. William Hotel at 8:00 AM. Additional vans and cars can meet at the first stop (North Pond/Swede Pond). The official trip begins at North Pond at 9:00 AM.

Most of the stops are road-side stops. It will be grassy, possibly wet, and as usual, there is potential for ticks, chiggers, mosquitos, etc.

Meeting Point (for those not meeting at the Fort William Hotel)

Meet at the parking area at the east end of North Pond on Rt.8, ~5mi west of Hague, NY. Note, there are two pull-offs, one at the east end and one near the western end of North Pond. The trip will meet at the east end pull-off. Park along the edges of the pull-off road.

The meeting point is also the first stop. We will have an introductory talk and then visit outcrops across Route 8. **UTM: NAD 83, 18T 0614217; 4844335**

Stop 1: North Pond/Swede Pond (Rt. 8, Hague, NY) -

Stop 1a. Dixon schist-marble-quartzite-khondalite

(Description partly taken from McLelland et al., 2002).

Rocks along Rt. 8 are dominated by metamorphosed sedimentary rocks; partially melted metapelitic rocks are particularly common. Bedding and a strong early foliation are shallowly dipping (east or west). Recumbent isoclinal folds have been described in a number of outcrops, including those at Stop-1. McLelland et al. (2002) described a large recumbent isoclinal fold at the southwestern end of the stop-1 outcrop. The fold axis plunges gently to the east or west and has been folded about upright E-W axial planes.

Rocks directly across from the pull-off are dominated by Dixon schist and marble. Dixon schist is a rusty slabby sulfidic rock that varies from garnet-bearing impure quartzite to garnet-rich schist. The more schistose varieties are similar to sillimanite-garnet-quartz-feldspar (khondalite) gneiss that we will see throughout the trip. Of particular note here is the strong mineral lineation on shallow, east-dipping foliation surfaces. The lineation plunges 20° => 090° on a foliation oriented 012°,21°.

Both Dixon schist and the khondalite were mined for flake graphite during the early part of the 20th century. The region around Swede Pond is known as the Dixon National Forest and the former mining hamlet of Graphite is located just to the East.

Stop-1b – Khondalite

Walk westward (carefully – traffic moves very fast!) along the road to the outcrops near the sign: “Parking Area 800 Ft.”). Most of the rocks along the way consist of shallowly-dipping Adirondack marble. This is a highly recrystallized, primarily calcite marble. Although the rocks are almost completely recrystallized, there are a number of very heterogeneous folds varying from isoclinal to open.

Just west of the “Parking Area 800 Ft.” is an excellent exposure of khondalite gneiss. The name “khondalite” originated in India, and refers to sillimanite-garnet-quartz-feldspar gneiss with notably little biotite. Sample 16TG-154 (Williams et al., this guidebook; Williams et al., in review) came from this outcrop. Here, the rock contains biotite, garnet, quartz, sillimanite, apatite, rutile, zircon, and monazite. Much of the biotite is interpreted to be a retrograde phase. K-feldspar is extremely abundant making up much of the matrix of the sample.

It occurs in continuous layers wrapping around garnet, forming strain shadows near garnet, and locally occurs as sigma-style porphyroclasts. Importantly, plagioclase is absent in the sample (Fig. 4).

The lack of peak biotite and plagioclase and the abundance of garnet and K-feldspar suggests that the following were important melting reactions.

$$Bt + Pl + Als + Qtz = Grt + Kfs + melt \quad (1)$$

$$Bt + Als + Qtz = Grt + Kfs + melt \quad (2)$$

Some initial melting may have been associated with muscovite dehydration, but modeling suggests that the amount of melting was probably limited (Storm and Spear, 2005; Yakumchuk and Brown, 2014). The complete lack of plagioclase suggests that Reaction-1 was exceeded. Peak conditions are interpreted to be in the range of 0.6-0.8 GPa, 700-800 °C based on phase relationships Storm and Spear, 2005; White et al., 2007; Yakumchuk and Brown, 2014) and also on calculated P-T conditions (Bohlen et al., 1985; Essene, Storm and Spear, 2005). We suggest that P-T conditions were within the region shown on Fig. 3.

The lack of plagioclase in sample 16TG-154 indicates that Reaction-1 was not significantly reversed during melt crystallization and retrograde metamorphism. The abundance of K-feldspar and garnet, similarly, suggests that Reaction-2 was not significantly reversed. Sample 16TG-154 does contain biotite, but at least some of this biotite may reflect late biotite growth associated with fluid influx long after melting. Because of the lack of reversal of the melting reactions and the lack of plagioclase-bearing leucosome, it seems likely that a significant portion of the melt component was removed from the local rock.

Monazite results. Figure 9 shows calculated monazite dates for sample 16TG-154 (see also Fig. 5). Figure 9 b,c shows Y-content in monazite vs. calculated date for the same sample. Arrows (Fig. 9c) connect core and rim analyses from single monazite grains. Figure 9d shows the sum of heavy rare earth elements (HREEs) in monazite vs. calculated date. HREEs and Y are strongly partitioned into garnet. The characteristic 'U-shaped' profiles in Figure 9 b,c,d are interpreted to result from significant garnet growth at ca. 1150 Ma and garnet breakdown after ca. 1000 Ma.

Figure 9e shows U content in monazite vs. calculated date. Like Y and HREEs, U decreases dramatically prior to 1150 Ma. However, unlike Y and HREEs, there is no late-stage increase in U. Partitioning data from Stepanov et al. (2012) indicate that the actinides (U, Th) have positive monazite/melt fractionation, but U has a significantly lower ratio than Th and most REEs. During partial melting U and other trace and REEs will be partitioned from the whole rock into melt. The decrease in U in monazite in sample 16TG-154 is thus, interpreted to result from partial melting of the sample. The fact that this reduction occurred at the same time as the Y and HREE reduction is consistent with melting by reactions 1 and 2. The fact that the U content of monazite remains low during cooling and during subsequent events is taken as evidence that a large component of the melt was removed from the local system.

Importantly, sample 16TG-154 shows little evidence for garnet growth or melting at ca. 1050 Ma, suggesting that little or no melting occurred in this sample during the Ottawan orogeny.

Return to vehicles. We will head west on Rt. 8.

Mileage

0 Head west on Rt. 8

1.7 Pull-off on left (south). Drive to the second entrance to the parking area and turn in facing East.

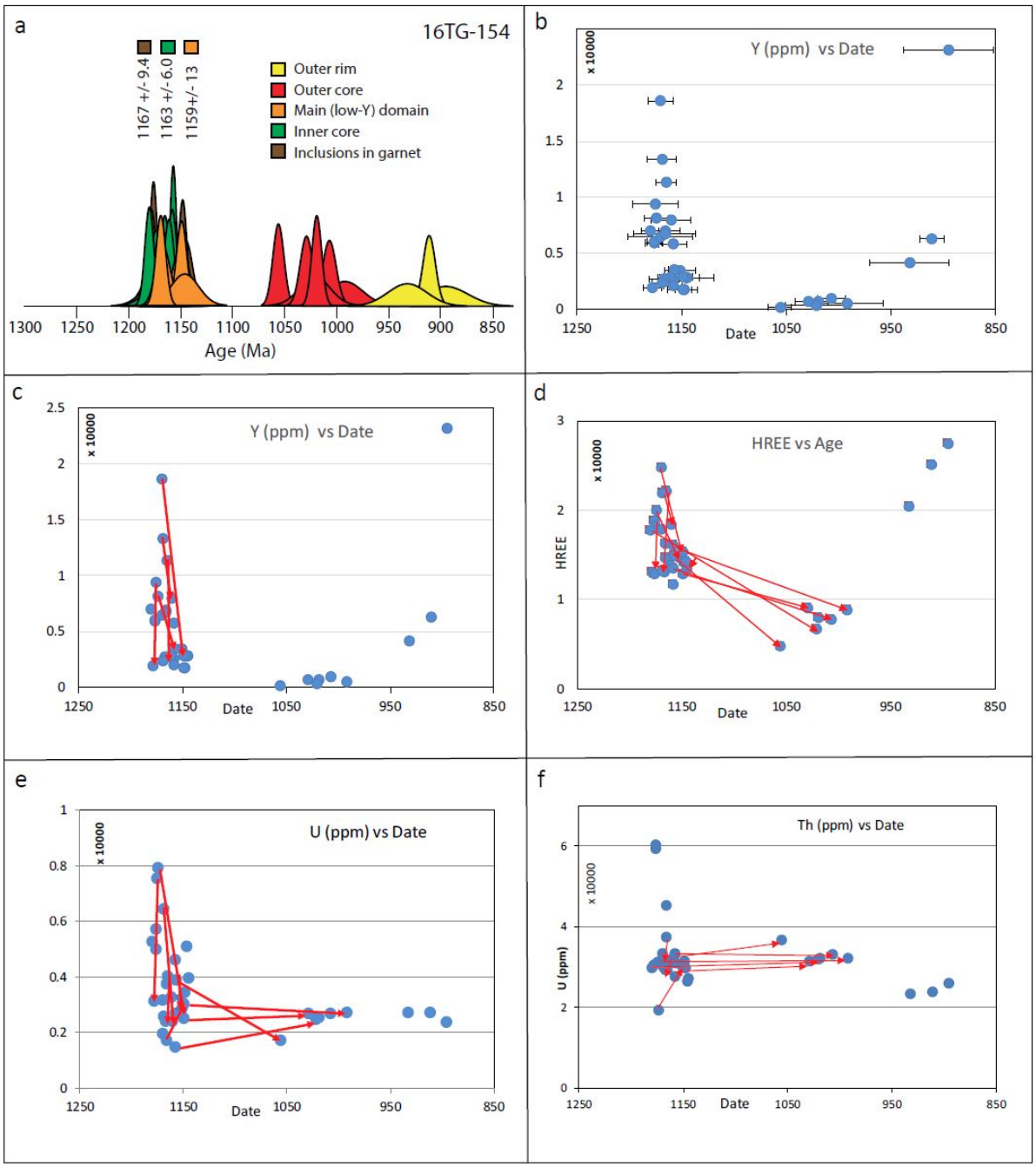

Figure 9. Monazite data from sample 16TG-154 North Pond - Swede Pond. See Figure 5 and text for discussion.

Stop 2. Treadway Mountain, UTM: 0612067; 4843537

A large outcrop of biotite-quartz-feldspar +/- sillimanite metapelite occurs along the north side of Rt. 8. Leucosome layers are abundant, ranging from centimeters to one meter in thickness. Similar to the North Pond outcrops, the foliation is shallowly dipping. Mineral lineations are poorly developed (preserved), but where present, trend to the east.

Several samples have been collected from this outcrop, including 16Tg151-a, b. In addition, this is Locality-9 from Bickford et al., 2008 (see below). The samples contain the common assemblage K-feldspar, garnet, quartz, sillimanite, with apatite, rutile, zircon, and monazite. Biotite is relatively abundant compared to samples from the previous stop. Most of the biotite is interpreted to be a retrograde phase, but some biotite may have been present at peak conditions. Samples contain both plagioclase and K-feldspar. The feldspars are fine to medium grained and are dispersed through the rock. Most samples have plagioclase richer and poorer layers, but distinct leucosome segregations with sharp boundaries are not present in the analyzed samples.

Monazite Results: Monazite date-composition relationships in sample 16TG-151 (Fig. 10) show some distinct differences from the North-Pond samples. Both Y and HREEs decrease significantly at ca. 1150 Ma, consistent with a significant period of garnet growth at this time (Fig.10 b, c, d). Yttrium and HREEs increase after 1000 Ma, consistent with garnet breakdown. However, there is considerably more variability in monazite composition at ca. 1050 Ma than in samples from Swede Pond. Importantly, several monazite grains show a distinct decrease in Y and HREEs at ca, 1050 Ma. This is interpreted to indicate a second period of garnet growth.

Uranium in sample 16TG-151 shows fairly little change from 1150 through 1050 Ma (Fig. 10e). There is some evidence for an averaging effect (that is, grain-to-grain variability decreases in younger monazite) and possibly a slight decrease in U is apparent after 1000 Ma. This is distinctly different from the trend in 16TG-154 where U was dramatically depleted at ca. 1150 Ma.

Two grains (M-3 and M-19) illustrate the behavior in this sample particularly well (Fig. 11, 12)). Monazite grain #3 has eight distinct domains (Fig. 11). HREEs drop at ca. 1150 from the innermost core to the next domain. HREES are relatively constant to the outermost core domain (1060 Ma) Then, there is a second decrease in Y and HREEs at approximately 1060-1050 Ma. This decrease is taken to be a second period of garnet growth at ca. 1050 Ma. The relatively constant Y and HREEs in grain 3 from 1150 to 1060 suggests that there was relatively little garnet growth (or breakdown?) during this 100 m.y. period. Grain 19 has no domains in the 1150 Ma range, but has at least nine domains that are ca. 1060 and younger (Fig. 12). This grain documents the progressive decrease in Y and HREEs at ca. 1050. The fact that U also decreases at this time is taken to indicate further melting, probably by a reaction such as reaction 1 and/or 2.

Return to Vehicles **Reset odometer to zero!**

Head east toward Hague, NY

1.7 North Pond pull-off (Stop-1)

2.5 Elephant Rock

We will discuss results from Elephant Rock, but will not make a stop. Parking is limited and the traffic can be heavy. See results in Williams et al., this guidebook; Williams et al., in review).

6.5 Town of Hague, NY

6.8 Turn left (north) on Rt. 9N

15.6 Intersection Rt. 9N and Montcalm St. Turn left toward 9N

16.3 Intersection Rt. 9N, Rt. 74 (west), and Rt. 22 (east). - Turn Left on Rt. 74

17.4 Pull off on right shoulder.

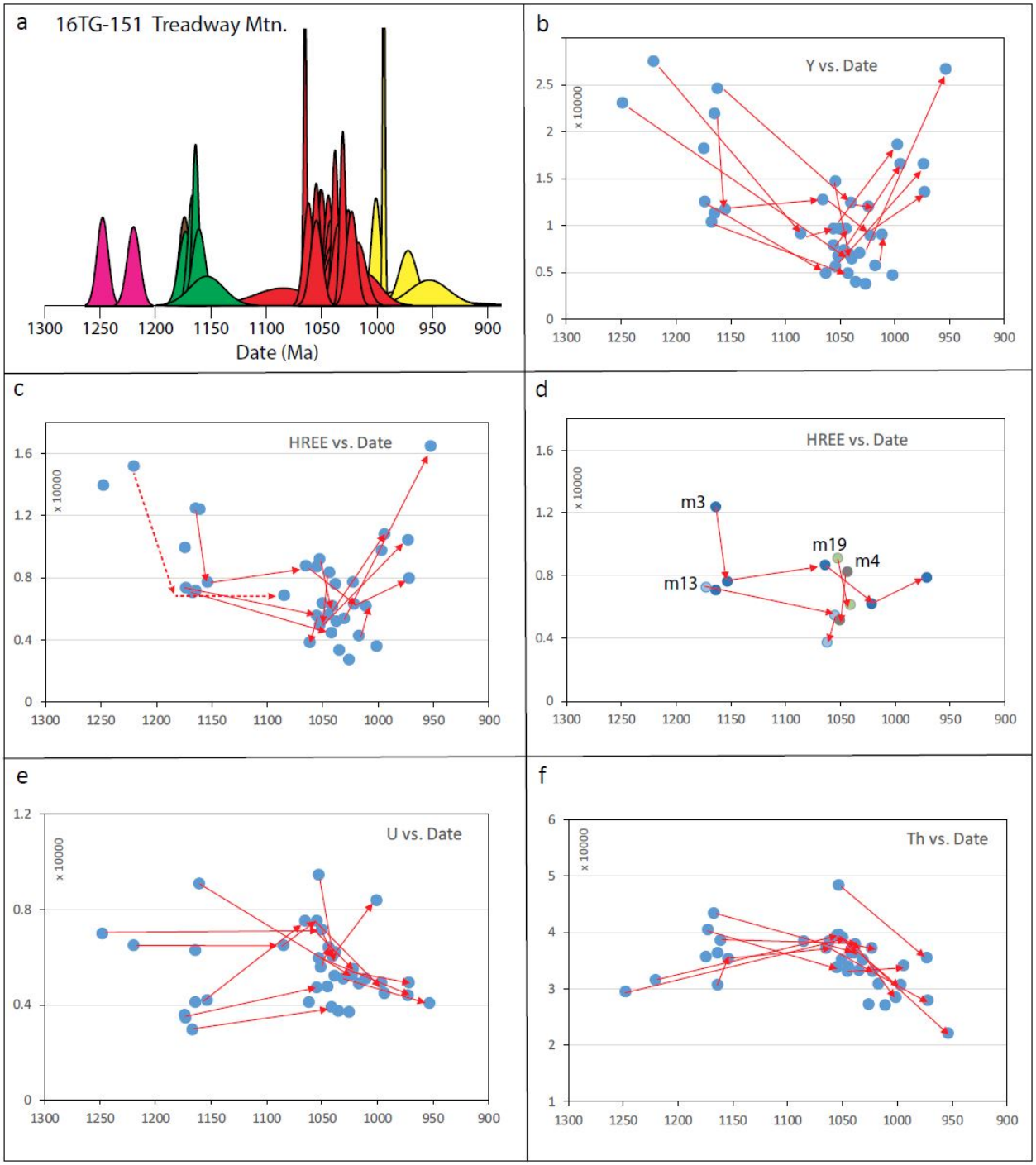

Figure 10. Monazite data from sample 16TG-151, Treadway Mountain outcrop, Rt. 8, Hague, NY. See text for discussion.

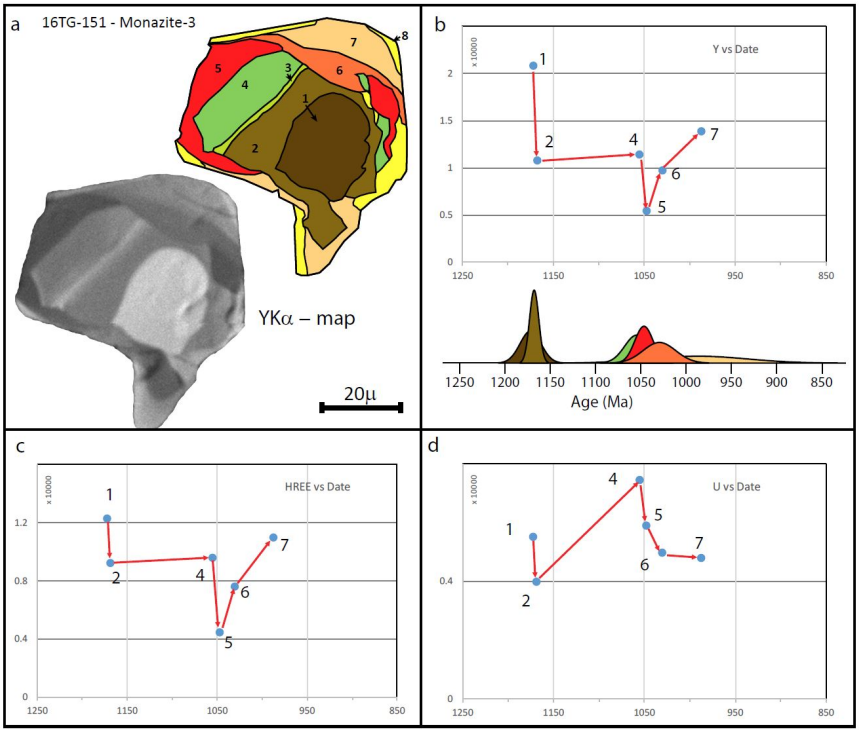

Figure 11. Monazite composition-date relationships from Monazite-3 from sample 16TG-151. See text for discussion.

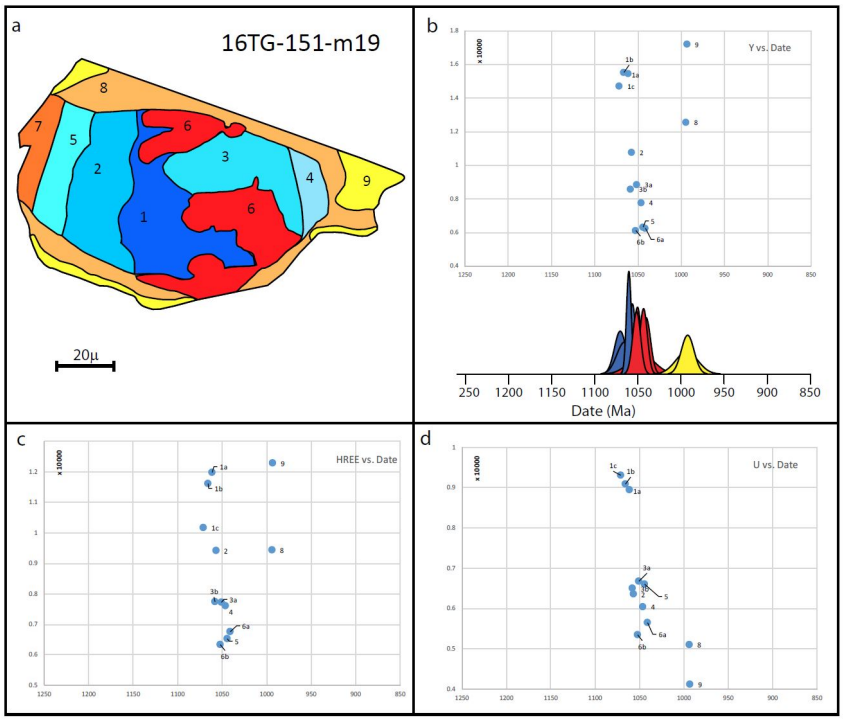

Figure12. Monazite composition-date relationships from Monazite-19 from sample 16TG-151. See text for discussion.

Stop 3. Roadcut on NY-74, west of Ticonderoga, NY

The easternmost rock at this outcrop is a poikiloblastic garnet amphibolite that contains garnet, clinopyroxene, plagioclase, and hornblende. Fe-Ti oxides are present as well, although they can only be seen in thin section. The garnet crystals can reach upwards of 3 cm in diameter. The best examples are concentrated in the westernmost part of the garnet amphibolite. Schistosity, mostly defined by aligned hornblende, appears to both traverse and wrap around the garnet poikiloblasts, suggesting garnet growth was syn-kinematic. Geochemistry of the amphibolite (Fig. 13) is consistent with other metamorphosed mafic members of the AMCG suite, constraining intrusion of the protolith to ca. 1160-1140 Ma.

Further west along the outcrop is a transition zone, marked by a vegetated slope, containing some layers of marble and a rusty weathering paragneiss. West of the transitions zone the vast majority of the outcrop is composed of a garnet-biotite-plagioclase-perthitic microcline-quartz ± sillimanite migmatitic paragneiss. Leucosome proportion is estimated to be 30-50%. Leucosomes preferentially contains garnet, while biotite is concentrated in the melanosome. Both leucosome and melanosome layers are deformed and define a foliation parallel to a schistosity defined by aligned biotite. Quartz and feldspar are granoblastic in both the leucosome and melanosome.

Within the migmatitic paragneiss are a number of garnet rich boudins. These are possibly deformed and metamorphosed dikes. The boudins indicate stretching in all directions parallel to gneissic layering suggesting a flattening finite strain. Also present within the migmatitic paragneiss are bodies of amphibolite similar to what is present at the east end of the outcrop. Three, 5 to 30 meters wide, unstrained, amoeboid-shaped, pegmatitic granitic plutons also occur in the migmatitic paragneiss.

The pegmatites contain feldspar, quartz, and biotite and are likely an alkali-feldspar granite, but some feldspars are striated. Locally associated with the pegmatites, the host migmatite contains cm-size books of graphite.

The fabric is essentially parallel among the garnet amphibolite, the migmatitic paragneiss, and the transitional contact zone (Fig. 14). The in the eastern half of the outcrop the foliation is ~062, 43 SE but changes to ~103, 45 SW by the westernmost end of the outcrop. A mineral lineation, defined by aligned hornblende, biotite, or sillimanite, depending on location, predominately plunges gently to the ESE (~20 → 100). This fabric is identified as the second regional fabric, forming after AMCG intrusion. Asymmetric tails on garnet poikiloblasts in the garnet amphibolite suggest top to the west transport.

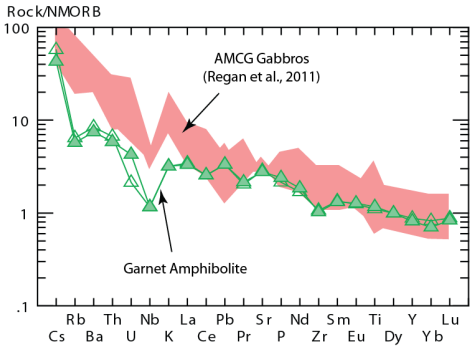

Figure 13. Multielement diagram (Sun and McDonough, 1989) for the garnet-amphibolite compared to other mafic members of the AMCG suite. Both are tholeiitic and have identical REE profiles.

Samples of the migmatitic paragneiss and of pegmatite were processed for U-Pb zircon geochronology (see also Regan et al., 2015). Presented here are preliminary results from a new sample that is solely of a structurally late migmatite leucosome that connects to adjacent leucosome boudinaged by S_2.

Two distinct generation of zircon can be identified in this sample by both CL and geochronology. Oscillatory zoned zircon with a bright CL response are found as cores within grains or forms entire grains. The most concordant, best cluster of ages for this zircon type provide a weighted $^{207}Pb/^{206}Pb$ age of ca. 1177 +/- 10 Ma (Fig. 15), interpreted to reflect zircon growth during Shawinigan migmatization, consistent with previous results from this outcrop. Oscillatory zircon with a dark CL response is found as rims surrounding the bright zircon or as entire grains. The oldest, concordant, tightly grouped analyses of this zircon produce a Concordia age of ca. 1067 +/- 6 Ma (Fig. 15), which is taken to be the age of a second, Ottawan-aged migmatization event and formation of the penetrative S_2 fabric.

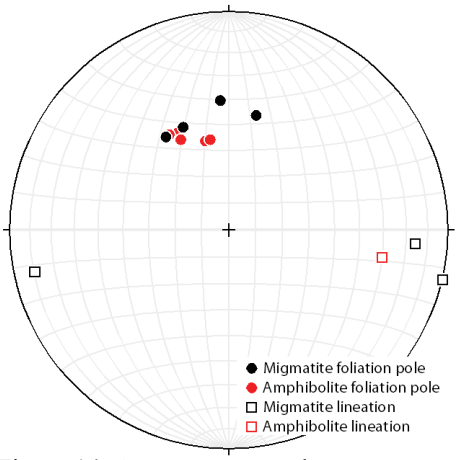

Figure 14. Outcrop structural pattern.

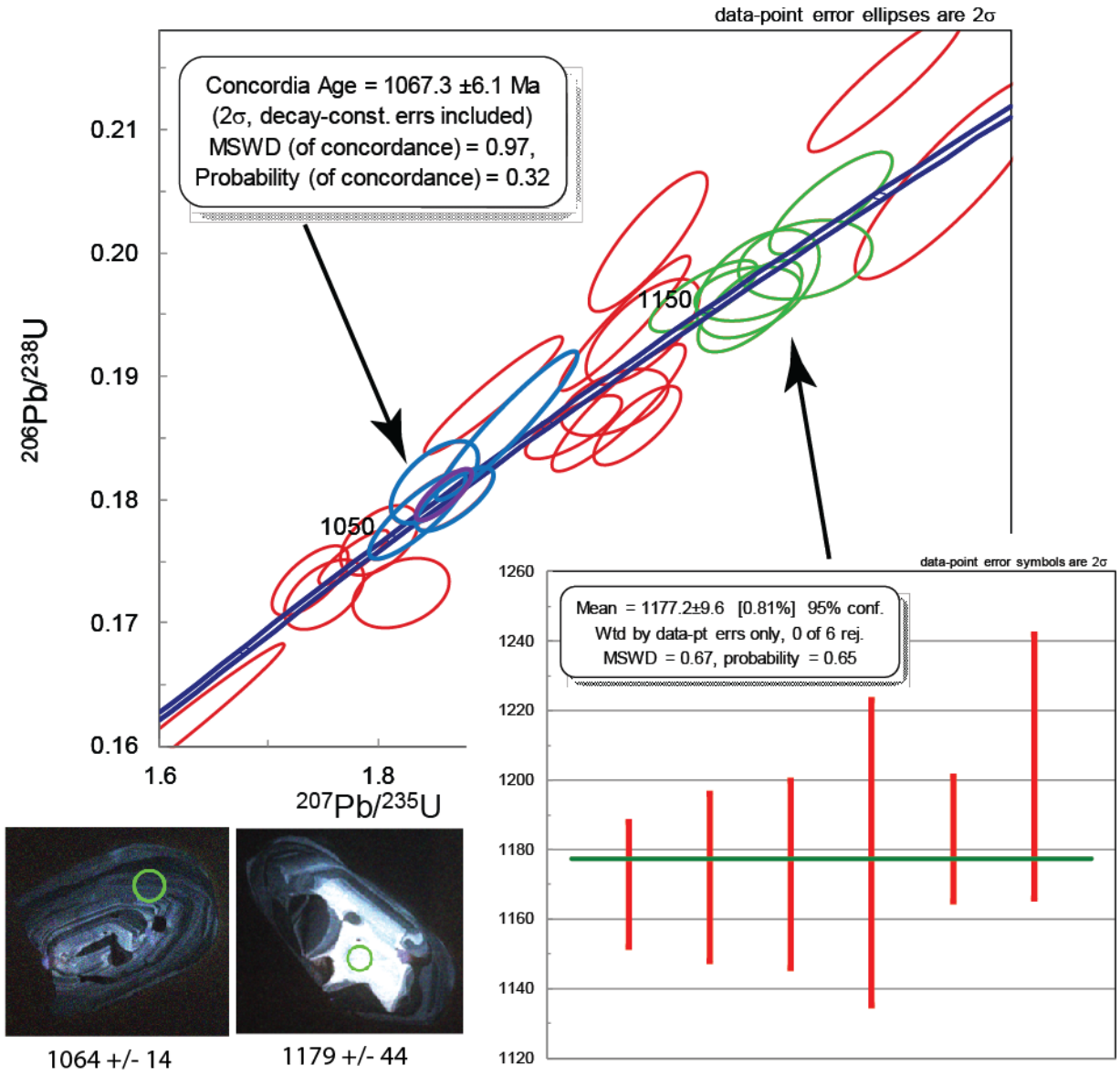

Figure 15. Concordia diagram for zircons isolated from the late-leucosome analyzed by LA-ICP-MS. Green analyses best date Shawinigan migmatization (weighted average given), blue analyses best date Ottawan migatization (Concordia age). Representative CL images and spot ages shown.

One pegmatite body produced uniform oscillatory or sector zoned zircon with a dark CL response. Nine analyses of this zircon are concordant or near concordant and produce a Concordia age of 1015 ± 10 Ma (Fig. 16), thought to best represent the age of pegmatite formation.

We have completed analyses of monazite from several samples from the migmatite. The overwhelming majority of monazite are ca. 1050 Ma and younger (Fig. 17), with only one small core domain yielding ca. 1150 date. Decreasing Y for some monazite grains (Fig. 18), the presence of ca. 1050 Ma monazite inclusions in garnet, and given the zircon data, demonstrate most monazite crystallization occurred late during or following Ottawan leucosome crystallization. Increasing Y in 1030 Ma and younger monazite supports garnet breakdown and retrograde metamorphism beginning at this time, as seen throughout the region. With the zircon data suggesting an earlier period of melting during the Shawinigan orogeny, it is likely that virtually all earlier monazite was consumed during this early or subsequent melting events. No age pattern is convincingly evident in the monazite U concentration, suggesting melt largely did not escape during either melting event (Fig. 18).

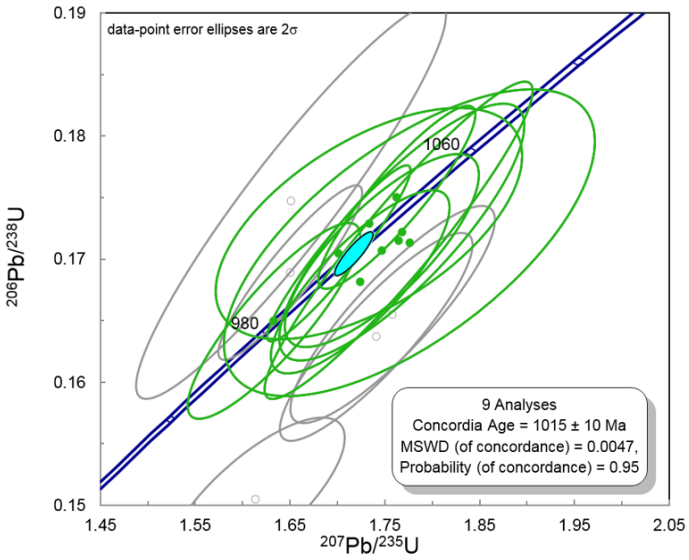

Figure 16. Concordia diagram for pegmatite zircon analyzed by SHRIMP-RG. Green analyses best date crystallization (Concordia age).

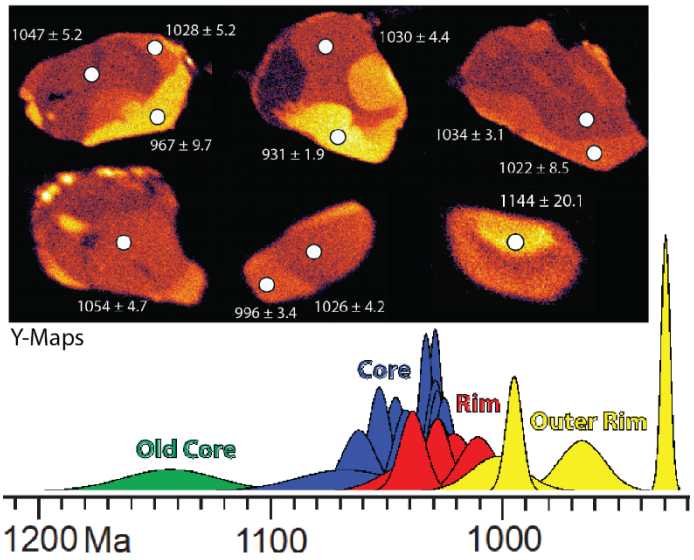

Figure 17. Summary of migmatite monazite ages with representative spot analyses.

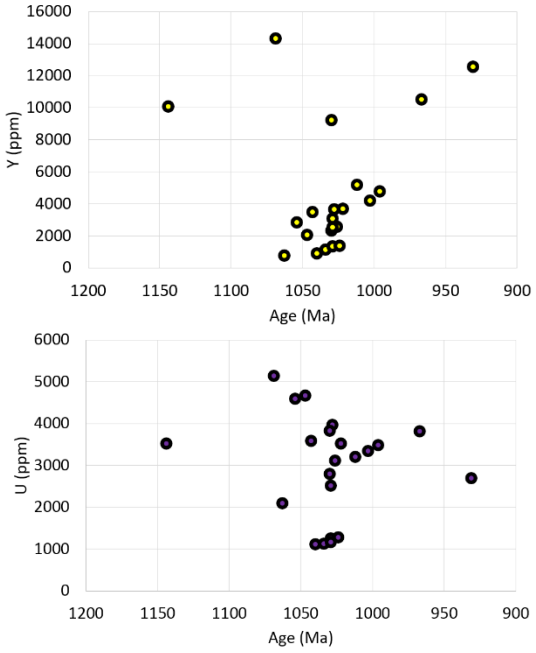

Figure 18. Monazite Y and U concentration.

Return to vehicles. Turn around (carefully) and return to intersection of Rt. 74, 9N, and 22.

Note Reset Trip Mileage to ZERO.

0 – Miles from Rt. 72-22 Intersection

At this point some cars may want to take a bathroom break at McDonalds or the Maplefield's gas station (northeast corner). The trip will collect at the rest-stop/lunch stop.

1.6 Blinking traffic light, intersection with east end of Montcalm St.

5.0 Turn into rest area on right.

This is a brief lunch stop, for those who bring lunch. People who stop for long in Ticonderoga may have to eat in vehicles on the way to the next stop!!

9.9 Putnam Station – note Cambrian Potsdam sandstone on right above the Great Unconformity

15.2 Turn right into Belden Road

15.4 Turn around at Manning Rd. and return on Belden Rd.

15.6 Park on right side of Belden Rd.

Stop 4. Dresden Station: Garnet-sillimanite gneisses and coronitic metagabbro (UTM 18 NAD83 - 628107 E, 4837420 N)

Many field trips have stopped at this location over the years. This description comes partly from Grover et al. (2015). McLelland et al. (1988a) used this outcrop to show that there were multiple phases of metamorphism recorded by the rocks in the Adirondacks. A sharp contact between garnet-sillimanite gneiss and a coronitic metagabbro is well-exposed in this outcrop (Fig. 19). The gneiss is a garnet-sillimanite-plagioclase-K-feldspar-quartz (khondalite) gneiss with a small amount of biotite. The khondalite is associated with quartzite and calc-silicate rocks as in many other parts of the Adirondacks.

The garnet-sillimanite gneiss is penetratively deformed with a well-developed foliation and a lineation that plunges gently to the east (21° => 091°). Much of the metagabbro is undeformed and a coarsely crystalline texture is preserved throughout much of the unit. There are places within the gabbro however that are deformed and foliated. Adjacent to the khondalite contact, the gabbro is fine grained (Fig 19c). It appears to coarsen toward the interior of the body, suggesting that a chilled margin formed at the contact. The contact between the gneiss and the gabbro is, in places, at a high angle to the foliation in the gneiss. These field relationships suggest that the gneiss was deformed and metamorphosed prior to the intrusion of the gabbro (McLelland et al., 1988).

Figure 19. Contact between garnet-sillimanite gneiss and coronitic metagabbro. Figure 19a shows that locally the foliation in the gneiss is parallel to the contact and locally it is at a high angle to the contact. Figure 19b illustrates the sharp nature of the contact. Figure 19c shows that the metagabbro is finely crystalline in the immediate vicinity of the contact.

Coronitic metagabbro bodies are found throughout the Adirondacks (Whitney and McLelland, 1973; Whitney and McLelland, 1983; Regan et al., 2011). Figure 20 illustrates the typical corona texture with an olivine core, surrounded by a rim of orthopyroxene, which in turn is rimmed by symplectic intergrowths of garnet and clinopyroxene. Ilmenite is typically rimmed by Ti-rich hornblende. Clouding in the plagioclase is due to microscopic spinel inclusions. This mineral assemblage and texture developed via subsolidus recrystallization from a rock that was originally an olivine-clinopyroxene-plagioclase gabbro. Preliminary P-T estimates suggest this mineral assemblage developed at approximately 9 kb and 750 °C. The growth of amphibole also requires an influx of an H_2O-bearing fluid.

To the south and west of this outcrop of gabbroic rocks, ferrogabbroic rocks and anorthosites, all thought to be associated with the metagabbro, have a very strong penetrative fabric and in many locations are mylonites. These rocks contain garnet, clinopyroxene, plagioclase, and local orthopyroxene, similar to the mineral assemblage found in the coronitic metagabbro. Kinematic indicators in these rocks suggest a west-directed thrust sense of motion. This period of deformation and metamorphism must postdate the emplacement of the AMCG rocks, but it is not clear if it reflects the late Shawinigan orogeny or the Ottawan orogeny. McLelland et al. (1988b) reported a U-Pb zircon, multigrain age of 1144 ± 7 Ma for the metagabbro. This is interpreted as an igneous crystallization age, consistent with the gabbro belonging to the AMCG suite. However, Aleinikoff and Walsh (2015) report a SHRIMP age of ca. 1134 +/- 3 Ma which suggests emplacement was during the waning stages of, or slight after the Shawinigan Orogeny.

We dated monazite from several samples of the garnet-sillimanite gneiss. The data fall into three broad populations (Fig. 6). The oldest population has a weighted mean of 1179 ± 9 Ma. We suggest that this represents the timing of prograde Shawinigan metamorphism. The next population yields ages that cluster around 1151 Ma. This is interpreted to represent the peak of metamorphism and melting driven by a thermal perturbation resulting from the intrusion of the gabbroic rocks. Most of the remaining monazite dates are 1020 Ma or less. These are too young to correlate with the proposed timing of the peak of the Ottawan Orogeny (~1090-1050 Ma). Instead, this generation probably represents post-Ottawan decompression and uplift.

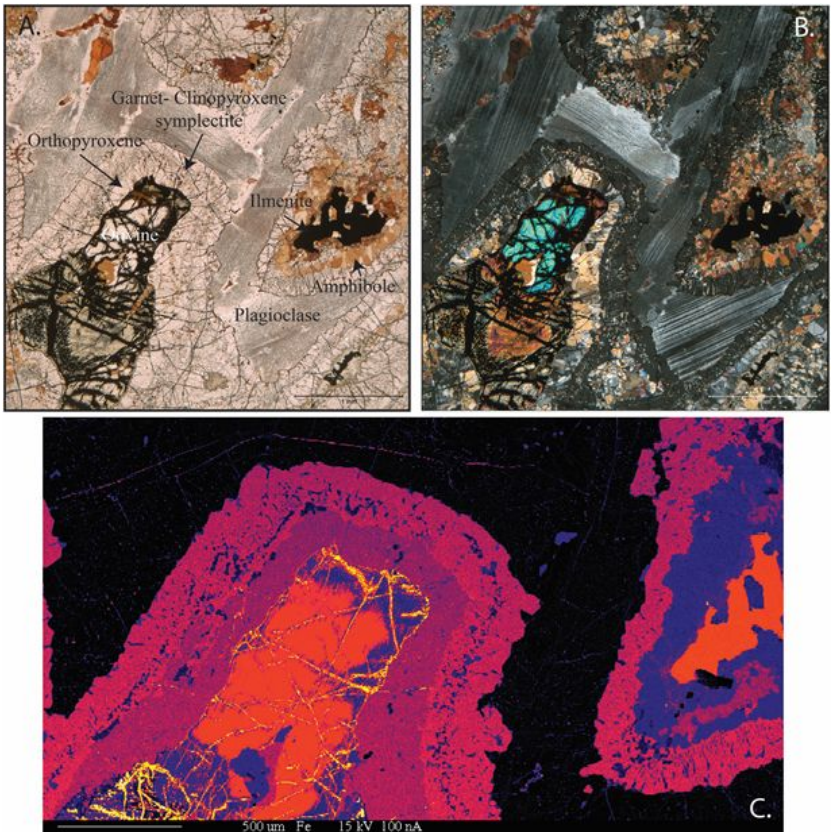

Figure 20. Photomicrographs and Fe-x-ray map of coronitic metagabro. Figure 20 a,b are photomicrographs under plane and cross polarized light respectively. Orthopyroxene surrounds olivine, and is in turn surrounded by garnet-clinopyroxene symplectite. Figure 20c is a Fe-Kα map of a portion of the thin section shown in 20 a,b.

The following model is consistent with the field observations and data from this outcrop. The mineral assemblage and the fabric in the garnet-sillimanite gneisses formed during the Shawinigan Orogeny. The gabbro was emplaced at approximately 1150 Ma, after the prominent fabric developed in the gneisses. This time frame is consistent with both the monazite dates from the gneisses and the multigrain age from the gabbro. Following the emplacement of the gabbro there was another period of deformation and metamorphism. This is when the nearby AMCG rocks were deformed and metamorphosed. This is also when the coronitic texture developed in the metagabbro. This requires in influx of an H_2O–bearing fluid. Unlike the nearby rocks, the coronitic metagabbro was not pervasively deformed at this time nor did any new monazite grow in the garnet-sillimanite gneiss. Perhaps strain was partitioned around this outcrop and the lack of strain resulted in little recrystallization in the largely anhydrous garnet-sillimanite gneisses. The 1020 Ma and younger monazite ages in the garnet-sillimanite gneisses record monazite growth during post Ottawan extensional collapse.

Return to vehicles and proceed south on Rt. 22.

25.0 Large outcrop of khondalite gneiss on right, referred to as "Whitehall khondalite"

26.9 Town of Whitehall; intersection of Rt. 22 and Rt.4. Continue south on Rt. 22.

33.0 Parking area on left

Be careful turning across traffic. Rt. 22 is busy and fast here!

Stop 5. Lineated Sillimanite Gneiss and the East Adirondack Shear Zone
Coordinates: UTM Z18 NAD83 (626163 E, 4813714 N)

Walk south (left) along Rt.22 to the first set of low outcrops.

Stop 5a. Sillimanite Gneiss. This outcrop contains interlayered garnet-biotite-sillimanite gneiss with greenish calc-silicate layers. The well exposed foliation surfaces of the sillimanite-bearing gneiss commonly have well-lineated, coarsely crystalline sillimanite. The lineation plunges gently to the southeast (18° => 130°). This lineation is distinctly different than that at the previous stops. It may represent a completely different stage of the tectonic history. These rocks are interpreted to have been affected by the East Adirondack shear zone (Wong et al., 2012), although kinematic indicators are better developed in outcrops just to the south (Stop 5b).

In-situ monazite analyses have been carried out as part of this work (Suarez et al., 2017) and also as part of the Wong et al (2012) study. Six distinct compositional populations (generations) have been recognized in the migmatitic metasedimentary samples: 1178 Ma, 1139 Ma, 1064 Ma, 1049 Ma, 1030 Ma, and ca. 1000 Ma (Fig. 8); see also Suarez et al. (2017). Uncertainties are on the order of 10-20m.y. (2σ). There is a distinct drop in Y and HREE between the ca. 1140 and ca. 1060 populations. An additional decrease occurs between the 1064 and 1049 Ma populations. Uranium also shows decreases in the 1060-1050 Ma range. Although work is still underway, there is little evidence in these rock for significant melting at ca. 1150 Ma. The data are consistent with the dominant melting event to have occurred at ca. 1060 Ma. The lowest Y and REE and U contents are associated with the ca. 1050 Ma population, suggesting that garnet growth and additional melting occurred at this time. It is possible that there was one prolonged melting event or alternatively melting may have occurred during the culmination of Ottawan shortening (1090-1060 Ma) and a second event associated with post Ottawan extension and intrusion of the Lyon Mountain granite (ca. 1050 Ma).

The 1030 Ma monazite population is interpreted to represent shearing associated with the East Adirondack shear zone (Wong et al., 2012). Y and HREE contents increase dramatically after 1050 Ma, probably reflecting garnet break-down during exhumation. The high(er)-Y overgrowths on monazite grains are commonly located along the foliation and in extensional quadrants of the grains, further supporting the connection between this monazite generation, extensional shearing, and exhumation (see Wong et al., 2012). This period of extension is synchronous with the extension along the Carthage-Colton shear zone (McLelland et al., 2001; Streepey et al., 2001; Johnson et al., 2004). Based on the extremely low Th-content, the youngest population (ca. 1000 Ma) is interpreted to represent monazite associated with fluid infiltration and hydrothermal alteration events.

Monazite is present in thin leucosome layers within the gray migmatitic gneiss and also in thicker leucosome layers in the outcrop. Monazite from a thin (~ 1 cm) leucosome layer yielded dates 1050 Ma and younger. Because monazite is expected to dissolve into partial melt, i.e. most partial melts are undersaturated in

monazite components (Kelsey et al. 2008; Yakymchuk and Brown 2014; Harley and Nandakumar, 2014), we interpret the ca.1050 date to be the time of crystallization of this leucosome layer. Monazite from larger, more discrete leucosomes also yielded ca. 1050 Ma dates. However, these monazite grains have much greater U-content than the gray gneiss or the thin leucosome. We suspect that these leucosomes represent injections of external partial melts that have fractionated and evolved to higher U contents.

We have carried out in-situ and bulk zircon (U-Pb) analysis of some rocks from this outcrop. Bulk separates from gray gneiss yielded only ca 1050 dates but in-situ samples of the gray gneiss yielded both ca. 1150 and ca. 1050 dates. We suspect that this reflects a sampling bias where only the larger monazite grains were recovered during mineral separation and these are dominated by the younger populations. An analysis of a zircon separate from the thin leucosome layer from which monazite was also analyzed, yielded both ~1150 and ~1050 dates. The older dates are interpreted to represent inherited zircon incorporated into the partial melt from the gray gneiss (see Suarez et al., 2017).

It is interesting to compare these data with that from stop 3. The monazite data from the stop 3 rocks had a strong Shawinigan, AMCG, and post Ottawan signature but virtually no peak Ottawan monazite growth. The monazite data from this outcrop have Shawinigan and Ottawan monazite populations, but the data suggest that melting occurred mainly during the Ottawan event(s).

Follow the outcrop to the south remaining on the east side of Highway 22 for the time being.

Stop 5b. East Adirondack Shear Zone.

Note the interlayer folds in the upper part of the road cut on the east (Fig. 21). This exposure illustrates an older foliation that was transposed into a new foliation. Perhaps this is an example of a Shawinigan S1 transposed into a younger Ottawan or post-Ottawan S2. Across the highway is an asymmetric mafic boudin with a long tail that continues to the south in the upper part of the road cut (Fig. 22). Although it is clear that the boudin was involved in a period of ductile deformation, the road cut is oriented almost at right angles to the lineation direction so it is difficult to use the boudin for kinematic analysis.

Figure 21. Interlayer folds in paragneiss along Hwy22 at Stop 5b. Red line traces some folds. Note hammer for scale.

The granitic rocks to the left of the mafic boudin in the picture below are mylonitic, LS-tectonites with megacrystic K-feldspar porphyroclasts Fig. 23). The prominent lineation plunges gently to the southeast. Data from this outcrop was cited by Wong et al. (2012) as evidence for the East Adirondack Shear Zone. They report a U-Pb zircon age obtained using the SHRIMP-RG at Stanford, of the granite in Figure 23 of ca. 1140 Ma. This date suggests that it is part of the AMCG suite and was emplaced towards the end or after the Shawinigan Orogeny.

Figure 22. Photomosaic of a mafic boudin enveloped by mylonitic, granitic gneiss at stop 5b. The mylonitic rocks pictured in Fig. 23 are located approximately in the center of this photo.

Following this reasoning they suggested that most of the strain in the rock is therefore related to Ottawan shortening or post Ottawan extension. They examined the asymmetric K-feldspar porphyroclasts as kinematic indicators to document shear sense motion. Although they found some porphyroclasts that suggested top to the west, thrust sense motion more suggest top to the east, normal-sense motion. They concluded that this rock experienced both early shortening (west-directed thrusting) and later extension.

Optional: cross the road and return to the vehicles along the west-side outcrops. This side gives an excellent view of the east-side outcrops, and to the north, there are excellent examples of coarse biotite-sillimanite-feldspar gneiss.

Be careful crossing the road. It is busy and fast.

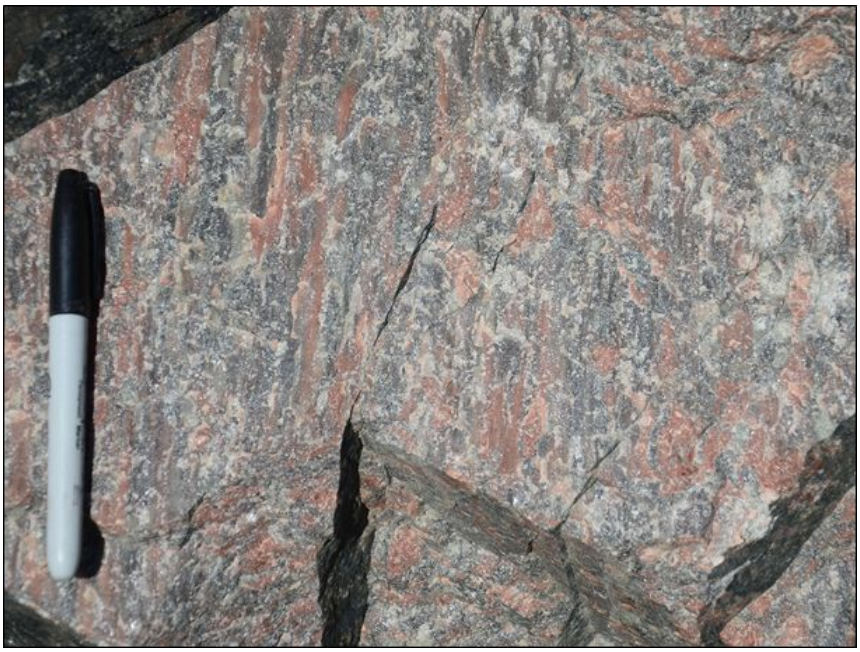

Figure 23. Strongly lineated granitic rock in the East Adirondack Shear zone.

Return to vehicles and continue south on Rt.4.

34.1 Turn right on Kelsey Pond Road.
Park on the side of the road. Carefully cross the highway to outcrop on the east side.

STOP 6. Mylonitic, Migmatitic "Straight" Gneiss

Coordinates UTM 18 NAD83: (625497 E, 4812086 N)

This is a beautiful exposure of a garnet-biotite-plagioclase-K-feldspar-quartz sillimanite gneiss. Most of the white layers are interpreted as leucosomes that formed during partial melting via a reaction such as Reaction-1. The strongly attenuated nature of the leucosomes, along with also remnants of pegmatite dikes that are now sheared into the foliation plane attest to the significant strain recorded by these rocks. The rocks have the same strong southeast-trending, gently plunging lineation that was seen at the last stop. We suggest that some of the strain in these rocks may be the result of post-Ottawan extensional collapse in the East Adirondack shear zone.

This outcrop was part of a study by Bickford et al. (2008). They concluded that these rocks underwent partial melting at approximately 1050 Ma at the tail end of the Ottawan Orogeny. They suggest anatexis was facilitated by an influx of H_2O-bearing fluids and decompression as a result of extensional collapse.

Figure 24 shows our preliminary U-Th-Pb electron microprobe monazite data from this outcrop. The data indicate monazite growth from approximately 1150 Ma through 1000 Ma with most monazite growth after 1100 Ma.

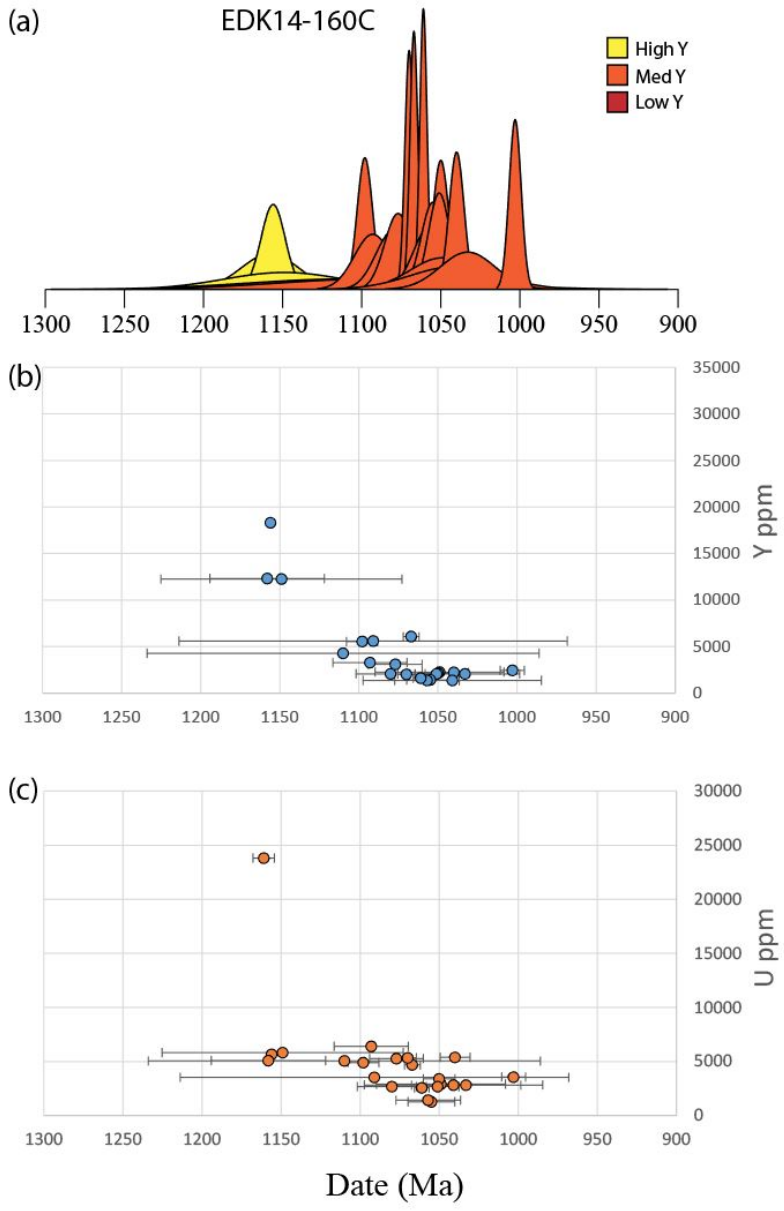

Figure 24. Monazite-composition data from the Rt. 22 "Straight Gneiss". (a) Dates from individual monazite domains; (b) Yttrium composition of monazite domains; (c) Uranium composition of monazite domains. See text for discussion.

Post-1100 Ma monazite have distinctly lower yttrium content than ca. 1150 monazite. The data are consistent with garnet growth and melting associated with the Ottawan orogeny and post Ottawan extension in agreement Bickford et al. (2008). However, there is also evidence for Shawinigan/AMCG monazite growth, and some suggestion that some melting may have occurred at this time. Combining these results with those of the precious stop, we see evidence for significant partial melting during Ottawan/post-Ottawan time. The extent of melting during Shawinigan/AMCG time is less certain, but the evidence from monazite or from zircon is certainly much less compelling. The may partly due to the intensity of the ca. 1050 Ottawan metamorphism, melting, and deformation, but we suspect that the earlier melting was much less extensive. Because the rocks were clearly fertile for melting during the later event, we suggest that Shawinigan temperatures were not sufficient for extensive biotite dehydration melting. This may reflect decreasing temperatures toward the outer parts of the Adirondack dome (as originally suggested by Bohlen et al., 1985). However, the observation that Shawinigan melting was synchronous with the AMCG plutonism suggests that the larger distance to AMGC gabbro and anorthosite may have contributed to higher temperatures during late Shawinigan time. We are in the process of collecting more data in order to further explore the effects of the Shawinigan and Ottawan Orogenies and post Ottawan orogenic collapse on these rocks.

End of Trip.

REFERENCES CITED

Allaz, J. M., Williams, M. L., J., J. M., Goemann, K., and Donovan, J., 2018- In Review, Multipoint Background Analysis: Gaining precision and accuracy in microprobe trace element analysis: Microscopy and Microanalysis.

Bickford, M.E., McLelland, J.M., Selleck, B.W., Hill, B.M., and Heumann, M.J., 2008, Timing of anatexis in the eastern Adirondack Highlands: Implications for tectonic evolution during ca. 1050 Ma Ottawan orogenesis: Geological Society of America Bulletin, v. 120, no. 7-8, p. 950–961.

Bohlen, S. R., Valley, J. W., and Essene, E. J., 1985, Metamorphism in the Adirondacks. I. Petrology, Pressure and Temperature: Journal of Petrology, v. 26, no. 4, p. 971-992.

Buddington, A. F., 1939, Adirondack igneous rocks and their metamorphism.: Geological Society of America Memoir - 7, 354p.

Chiarenzelli, J., Regan, S., Peck, W.H., Selleck, B.W., Cousens, B., Baird, G.B., and Shrady, C.H., 2010, Shawinigan arc magmatism in the Adirondack Lowlands as a consequence of closure of the Trans-Adirondack backarc basin: Geosphere, v. 6, no. 6, p. 900–916, doi: 10.1130/GES00576.1.

Chiarenzelli, J., Lupulescu, M., Thern, E., and Cousens, B., 2011, Tectonic implications of the discovery of a Shawinigan ophiolite (Pyrites Complex) in the Adirondack Lowlands: Geosphere, v. 7, no. 2, p. 333–356, doi: 10.1130/GES00608.1.

Chiarenzelli, J., Selleck, B., Lupulescu, M., Regan, S., Bickford, M. E., Valley, P., and McLelland, J. M., 2017, Lyon Mountain ferroan leucogranite suite: Magmatic response to extensional thinning of overthickened crust in the core of the Grenville orogen: GSA Bulletin, v. 129, no. 11-12, p. 1472-1488.

Gehrels, G. E., Valencia, V. A., and Ruiz, J., 2008, Enhanced precision, accuracy, efficiency, and spatial resolution of U-Pb ages by laser ablation–multicollector–inductively coupled plasma–mass spectrometry: Geochemistry, Geophysics, Geosystems, v. 9, no. 3.

Harley, S. L., and Nandakumar, V., 2014, Accessory Mineral Behaviour in Granulite Migmatites: a Case Study from the Kerala Khondalite Belt, India: Journal of Petrology, v. 55, no. 10, p. 1965-2002.

Harlov, D. E., and Hetherington, C. J., 2010, Partial high-grade alteration of monazite using alkali-bearing fluids: Experiment and nature: American Mineralogist, v. 95, no. 7, p. 1105-1108.

Harlov, D. E., Wirth, R., and Hetherington, C. J., 2011, Fluid-mediated partial alteration in monazite: the role of coupled dissolution–reprecipitation in element redistribution and mass transfer: Contributions to Mineralogy and Petrology, v. 162, no. 2, p. 329-348.

Heumann, M., Bickford, M., Hill, B., McLelland, J., Selleck, B., and Jercinovic, M., 2006, Timing of anatexis in metapelites from the Adirondack lowlands and southern highlands: A manifestation of the Shawinigan orogeny and subsequent anorthosite-mangerite-charnockite-granite magmatism: Bulletin of the Geological Society of America, v. 118, no. 11-12, p. 1283.

Jercinovic, M. J., Williams, M. L., and Lane, E., D., 2008, In-situ trace element analysis of monazite and other fine-grained accessory minerals by EPMA: Chemical Geology, v. 254, p. 197-215.

Jercinovic, M. J., Williams, M. L., and Snoeyenbos, D. R., 2008, Improved analytical resolution and sensitivity in EPMA – Some initial results from the Ultrachron development project: Microscopy and Microanalysis 14, supplement 2, p. 1272-1273.

Karlstrom, K. E., Harlan, S. S., Williams, M. L., McLelland, J., Geissman, J. W., and Ahall, K. I., 1999, Refining Rodinia; geologic evidence for the Australia-Western U.S. connection in the Proterozoic: GSA Today, v. 9, no. 10, p. 1-7.

Kelsey, D. E., Clark, C., and Hand, M., 2008, Thermobarometric modelling of zircon and monazite growth in melt-bearing systems; examples using model metapelitic and metapsammitic granulites: Journal of Metamorphic Geology, v. 26, no. 2, p. 199-212.

McLelland, J., Chiarenzelli, J., Whitney, P., and Isachsen, Y., 1988a, U-Pb zircon geochronology of the Adirondack Mountains and implications for their geologic evolution: Geology, v. 16, no. 10, p. 920–924, doi: 10.1130/0091-7613(1988)016<0920:UPZGOT>2.3.CO;2.

McLelland, J., Lochhead, A., and Vyhnal, C., 1988b, Evidence for multiple metamorphic events in the Adirondack Mountains, NY: The Journal of Geology, doi: 10.2307/30068728.

McLelland, J., Daly, J. S., and McLelland, J. M., 1996, The Grenville orogenic cycle (ca. 1350-1000 Ma); an Adirondack perspective: Tectonophysics, v. 265, no. 1-2, p. 1-28.

McLelland, J., Hamilton, M., Selleck, B., Walker, D., and Orrell, S., 2001, Zircon U-Pb geochronology of the Ottawan orogeny, Adirondack highlands, New York: regional and tectonic implications: Precambrian Research, v. 109, no. 1, p. 39–72.

McLelland, J. M., Bickford, M. E., Spear, F. S., and Storm, L. C., 2002, Geology and Geochronology of the Eastern Adirondacks: New York State Geological Association Field Trip Guide, Trip B1.

McLelland, J. M., Bickford, M. E., Hill, B. M., Clechenko, C. C., Valley, J. W., and Hamilton, M. A., 2004, Direct dating of Adirondack massif anorthosite by U-Pb SHRIMP analysis of igneous zircon: Implications for AMCG complexes: GSA Bulletin, v. 116, no. 11-12, p. 1299-1317.

McLelland, J., Selleck, B., Hamilton, M., and Bickford, M., 2010, Late-To Post-Tectonic Setting of Some Major Proterozoic Anorthosite–Mangerite–Charnockite–Granite (AMCG) Suites: Canadian Mineralogist, v. 48.

McLelland, J.M., Selleck, B.W., and Bickford, M.E., 2013, Tectonic Evolution of the Adirondack Mountains and Grenville Orogen Inliers within the USA: Geoscience Canada, v. 40, no. 4, p. 318, doi: 10.12789/geocanj.2013.40.022.

Mezger, K., 1992, Temporal evolution of regional granulite terranes: Implications for the formation of lowermost continental crust, *in* Fountain, D. M., Arculus, R., and Kay, R. W., eds., Continental Lower Crust: Amsterdam, Elsevier, p. 447-478.

Peck, W. H., Selleck, B., Regan, S., Howard, G. E., and Kozel, O. O., 2018, in Revision, In-situ dating of metamorphism in Adirondack anorthosite: American Mineralogist - Preprint.

Putnis, A., and Austrheim, H., 2010, Fluid-induced processes: metasomatism and metamorphism: Geofluids, v. 10, no. 1-2, p. 254-269.

Regan, S.P., Chiarenzelli, J.R., and McLelland, J.M., 2011, Evidence for an enriched asthenospheric source for coronitic metagabbros in the Adirondack Highlands: …,, doi: 10.1130/GES00629.1.

Regan, S., Walsh, G. J., Williams, M. L., Chiarenzelli, J. R., Toft, M., and McAleer, R. J., 2018, in Review, Syn-collisional exhumation of hot middle crust in the Adirondack Mountains: implications for extensional orogenesis in the southern Grenville Province: Geosphere.

Rivers, T., 2008, Assembly and preservation of lower, mid, and upper orogenic crust in the Grenville Province--Implications for the evolution of large hot long-duration orogens: Precambrian Research, v. 167, no. 3-4, p. 237–259.

Selleck, B., McLelland, J. M., and Bickford, M. E., 2005, Granite emplacement during tectonic exhumation: The Adirondack example: Geology, v. 33, no. 10, p. 781-784.

Spear, F. S., and Markussen, J. C., 1997, Mineral Zoning, P–T–X–M Phase Relations, and Metamorphic Evolution of some Adirondack Granulites, New York*: Journal of Petrology, v. 38, no. 6, p. 757-783.

Stepanov, A. S., Hermann, J., Rubatto, D., and Rapp, R. P., 2012, Experimental study of monazite/melt partitioning with implications for the REE, Th and U geochemistry of crustal rocks: Chemical Geology, v. 300–301, p. 200-220.

Storm, L. C., and Spear, F. S., 2005, Pressure, temperature and cooling rates of granulite facies migmatitic pelites from the southern Adirondack Highlands, New York: Journal of Metamorphic Geology, v. 23, no. 2, p. 107-130.

Suarez, K., Williams, M. L., Grover, T. W., and Pless, C. R., 2017, Constraining the Timing of Melting in the Eastern Adirondack Mountains, NY Using a Combination of In-Situ Monazite and Zircon U/Pb Dating Techniques: Geological Society of America Abstracts with Programs, v. 49, no. 6.

Suarez, K., 2018, Constraining the Timing of Melting in the Eastern Adirondack Mountains [MS: University of Massachusetts – In Progress.

Valley, J. W., and O'Neil, J. R., 1982, Oxygen isotope evidence for shallow emplacement of Adirondack anorthosite: Nature, v. 300, p. 497.

Valley, P. M., Fisher, C. M., Hanchar, J. M., Lam, R., and Tubrett, M., 2010, Hafnium isotopes in zircon: A tracer of fluid-rock interaction during magnetite–apatite ("Kiruna-type") mineralization: Chemical Geology, v. 275, no. 3, p. 208-220.

Valley, P.M., Hanchar, J.M., and Whitehouse, M.J., 2011, New insights on the evolution of the Lyon Mountain Granite and associated Kiruna-type magnetite-apatite deposits, Adirondack Mountains, New York State: Geosphere, v. 7, no. 2, p. 357–389, doi: 10.1130/GES00624.1.

Walsh, G.J. and Aleinikoff, J.N, 2016, New U-Pb zircon ages and field studies support Shawinigan deformation in the Eastern Adirondacks: Geological Society of America Abstracts with Programs, v. 48, no. 2.

White, R. W., and Powell, R., 2002, Melt loss and the preservation of granulite facies mineral assemblages: Journal of Metamorphic Geology, v. 20, no. 7, p. 621-632.

White, R. W., Powell, R., and Holland, T. J. B., 2007, Progress relating to calculation of partial melting equilibria for metapelites: Journal of Metamorphic Geology, v. 25, no. 5, p. 511-527.

Williams, M.L., Jercinovic, M.J., Goncalves, P., and Mahan, K., 2006, Format and philosophy for collecting, compiling, and reporting microprobe monazite ages: Chemical Geology, v. 225, no. 1-2, p. 1–15, doi: 10.1016/j.chemgeo.2005.07.024.

Williams, M.L., Jercinovic, M.J., and Hetherington, C.J., 2007, Microprobe Monazite Geochronology: Understanding Geologic Processes by Integrating Composition and Chronology: Annual Review of Earth and Planetary Sciences, v. 35, no. 1, p. 137–175, doi: 10.1146/annurev.earth.35.031306.140228.

Williams, M. L., Jercinovic, M. J., Harlov, D. E., Budzyn, B., and Hetherington, C. J., 2011, Resetting monazite ages during fluid-related alteration: Chemical Geology, v. 283, no. 3-4, p. 218-225.

Williams, M. L., Jercinovic, M. J., Mahan, K. E., and Dumond, G., 2017, Electron microprobe petrochronology, *in* Kohn, M. J., Engi, M., and Lanari, P., eds., Petrochronology: Methods and Applications, Volume 83, Reviews in Mineralogy and Geochemistry v. 83 p. 153-182.

Williams, M. L., Grover, T. W., M.J., J., Regan, S., Pless, C. R., and Suarez, K., 2018-In Preparation, Constraining the timing and character of extreme crustal melting in the Adirondack Mountains using multiscale compositional mapping and in-situ geochronology.

Wong, M.S., Williams, M.L., McLelland, J.M., Jercinovik, M.J., and Kowalkoski, J., 2012, Late Ottawan extension in the eastern Adirondack Highlands: Evidence from structural studies and zircon and monazite geochronology: Geological Society of America Bulletin, v. 124, no. 5-6, p. 857–869, doi: 10.1130/B30481.1.

Yakymchuk, C., and Brown, M., 2014, Behaviour of zircon and monazite during crustal melting: Journal of the Geological Society, v. 171, no. 4, p. 465-479.

Yakymchuk, C., 2017, Behaviour of apatite during partial melting of metapelites and consequences for prograde suprasolidus monazite growth: Lithos, v. 274–275, p. 412-426.